

## NEUROSYSTEMS

# Nonassociative plasticity alters competitive interactions among mixture components in early olfactory processing

Fernando F. Locatelli,<sup>1,\*</sup> Patricia C. Fernandez,<sup>1,†</sup> Francis Villareal,<sup>1</sup> Kerem Muezzinoglu,<sup>2</sup> Ramon Huerta,<sup>2</sup> C. Giovanni Galizia<sup>3</sup> and Brian H. Smith<sup>1,\*</sup>

<sup>1</sup>School of Life Sciences, Arizona State University, PO Box 874501, Tempe, AZ, 85287, USA

<sup>2</sup>Biocircuits Institute, University of California, San Diego, La Jolla, CA, USA

<sup>3</sup>Department of Biology, University of Konstanz, Konstanz, Germany

**Keywords:** antennal lobe, learning, olfaction, plasticity

## Abstract

Experience-related plasticity is an essential component of networks involved in early olfactory processing. However, the mechanisms and functions of plasticity in these neural networks are not well understood. We studied nonassociative plasticity by evaluating responses to two pure odors (A and X) and their binary mixture using calcium imaging of odor-elicited activity in output neurons of the honey bee antennal lobe. Unreinforced exposure to A or X produced no change in the neural response elicited by the pure odors. However, exposure to one odor (e.g. A) caused the response to the mixture to become more similar to that of the other component (X). We also show in behavioral analyses that unreinforced exposure to A caused the mixture to become perceptually more similar to X. These results suggest that nonassociative plasticity modifies neural networks in such a way that it affects local competitive interactions among mixture components. We used a computational model to evaluate the most likely targets for modification. Hebbian modification of synapses from inhibitory local interneurons to projection neurons most reliably produced the observed shift in response to the mixture. These results are consistent with a model in which the antennal lobe acts to filter olfactory information according to its relevance for performing a particular task.

## Introduction

Animals must be able to perceptually filter out stimuli that are not relevant for survival. In general, infrequent stimuli are more informative than stimuli that are common (Shannon, 1948). For example, when faced with regular exposure to a stimulus that is not associated with an important consequence, such as food or a painful stimulus, animals typically decrease responsiveness to that stimulus. The decrease is defined as ‘habituation’ when the behavioral response to the stimulus is innate and the decrease can be not explained by motor fatigue. For example, rats and mice investigate a new odor at first, but the intensity of investigation wanes with repeated exposure (Hunter & Murray, 1989; Cleland *et al.*, 2002). Fruit flies show innate avoidance behavior to certain odors but the behavior habituates after massive sustained exposure (Das *et al.*, 2011). A related case of nonassociative learning is latent inhibition (Lubow, 1973). In contrast to habitua-

tion, animals are repeatedly exposed to a stimulus that does not at first elicit a behavioral response. Latent inhibition becomes evident only when the pre-exposed stimulus is subsequently associated with reinforcement in conditions that usually produce a robust conditioned response. For example, after regular exposure to an odor honey bees are slow to develop a conditioned response to that odor relative to other odors (Chandra *et al.*, 2010).

The neural mechanisms that underlie olfactory nonassociative learning and memory have received relatively less attention than the mechanisms for pavlovian and operant conditioning. However, there is indication that the mechanisms for nonassociative learning are complex and distributed in the brain. In mammals, components of this plasticity can be found in early olfactory processing in the olfactory bulb and piriform cortex (Wilson & Linster, 2008). At least part of the neural mechanism responsible for short-term olfactory habituation lies in a homosynaptic depression of transmission from second-order mitral cells in the olfactory bulb to their targets in the piriform cortex, and it depends on glutamate receptors on axon terminals of the mitral cells (Linster *et al.*, 2009). Prolonged or repeated exposure to odor produces habituation that depends on NMDA receptors in the olfactory bulb network (Wilson & Linster, 2008).

Neural networks involved in early olfactory processing are functionally similar in insects and mammals (Hildebrand & Shepherd, 1997; Strausfeld & Hildebrand, 1999). Furthermore, this similarity is most likely due to convergent evolution (Strausfeld & Hildebrand, 1999), which indicates that these neural networks reflect fundamental

*Correspondence:* Brian H. Smith, as above.  
E-mail: brian.h.smith@asu.edu

\*Present address: Laboratorio de Neurobiología de la Memoria, Departamento de Fisiología, Biología Molecular y Celular, Facultad de Ciencias Exactas y Naturales, Universidad de Buenos Aires, IFIByNE (UBA CONICET), Ciudad Universitaria, Buenos Aires, 1428EHA, Argentina

†Present address: INTA, EEA Delta del Paraná (UBA CONICET), Rio Paraná de las Palmas y Canal Comas, Campana, 2804, Argentina

Received 28 February 2012, revised 7 September 2012, accepted 13 September 2012

and broadly applicable solutions for olfactory encoding and plasticity. However, this similarity remains to be thoroughly investigated, particularly in regard to different types of plasticity. Here we investigate whether odor exposure that is sufficient to produce latent inhibition in the honey bee induces nonassociative modification of the neural networks in the antennal lobe (AL), which is the functional analog to the mammalian olfactory bulb. Using calcium imaging, we show that after regular presentation of an odor the neural representation of that odor is reduced in its ability to compete with that of a new odor when both are presented in a mixture. This result implies that network-level interactions in the AL are modified by unreinforced exposure. Furthermore, we show that this competition is reflected in behavioral overshadowing experiments. Finally, we use a computational model of the AL to predict specific synaptic changes that modify competitive interactions in the network with the same results as observed experimentally. Among the three conceivable hypotheses tested, the simplest one, namely Hebbian plasticity on inhibitory synapses towards the excitatory units, is the most likely mechanism.

## Materials and methods

### Animals

Honey bee (*Apis mellifera carnica*) pollen foragers (all female) were collected at the entrance of the colony, briefly cooled and restrained in individual Plexiglas stages suited for olfactory conditioning and optical recordings (Galizia & Vetter, 2004). After recovery from cooling, bees were fed 2 µL of a 1.0-M sucrose solution and remained undisturbed until staining or until further feeding. All imaging and behavior experiments were performed 1 day after capturing and restraining the animals.

### Projection neuron staining

The head was fixed to the Plexiglas stage with soft dental wax (Kerr; Sybron Dental Specialties, USA) in such a way that animals could freely move antennae and proboscis. A rectangular window was cut in the head capsule dorsal to the joints of the antennae and ventral to the medial ocellus. The glands were carefully moved aside until the alpha-lobe in the brain were visible; these are easily recognisable and serve as spatial reference to guide staining. Projection neurons (PNs) were stained by backfilling with the calcium sensor dye FURA-dextran (potassium salt, 10 000 MW; Invitrogen, Eugene, OR, USA). The tip of a glass electrode was coated with a bolus (approximately 50 µm diameter) of fura-dextran prepared in 3% bovine serum albumin solution (Sigma-Aldrich, St Louis, MO, USA). The coated electrode was inserted into both sides of the protocerebrum dorsolateral to the alpha-lobe where the antennoprotocerebral tracts run between the medial and lateral calyxes of the mushroom bodies (Kirschner *et al.*, 2006). Medial and lateral ACTs contain the axons of uniglomerular PNs (Abel *et al.*, 2001). The dye bolus dissolved into the tissue in 3–5 s and the window was immediately closed using the same piece of cuticle that had previously been removed. Eicosane (Sigma-Aldrich) was used to glue and seal the cuticle. Twenty minutes after staining the bees were fed again until satiation with 1 M sucrose and left undisturbed until next day. The dye was left to travel along the tracts for at least 12 h. Before imaging, the antennae were fixed pointing towards the front using eicosane, and body movements were prevented by gently compressing the abdomen and thorax with a piece of foam. The brain was rinsed with Ringer solution (in mM: NaCl, 130; KCl, 6; MgCl<sub>2</sub>, 4; CaCl<sub>2</sub>, 5; sucrose, 160; glucose, 25; and HEPES, 10; pH 6.7, 500 mOsmol; all chemicals from Sigma-Aldrich) and glands and trachea cover-

ing the ALs were removed. The ALs were examined for appropriate staining and only animals that by visual inspection presented homogeneous staining of all visually accessible glomeruli were used for experiments. To prevent brain movements during measurements a second hole was cut ventrally to the antennae, and the compact structure of muscles, esophagus and supporting chitin was lifted and put under slight tension (Maelshagen, 1993). Finally, the brain was covered with Kwik-sil (WPI) to further prevent movements and avoid desiccation during the experiment. After surgery animals were mounted in the microscope and were allowed to recover for 20 min before imaging.

### Imaging

Calcium imaging was done using a CCD camera (SensiCamQE; TILL Photonics, Germany) mounted on an upright fluorescence microscope (Olympus BX-50WI, Japan) equipped with a 20× dip objective, NA 0.95 (Olympus), 505 DRLPXR dichroic mirror and 515 nm LP filter (TILL Photonics). Monochromatic excitation light provided by a PolichromeV (TILL Photonics) alternated between 340 and 380 nm. Fluorescence was detected at a sampling rate of 5 Hz. Spatial resolution was 172 × 130 pixels binned on chip from 1376 × 1040 pixels, resulting in a spatial sampling of 2.6 µm per pixel side. Exposure times were 8 and 2 ms for 340 and 380 nm excitation light, respectively.

Animals underwent four imaging sessions, with an odor exposure session between the first and second imaging sessions (Fig. 2A). Each imaging session included six measurements of odor-induced activity in the AL: two measurements each of 1-hexanol, 2-octanone and the binary mixture 1 : 1. The six measurements were presented in random order and were separated by 1-min intervals. Ten minutes after the end of the first imaging session animals underwent an odor exposure session that lasted 40 min. The exposure session consisted of 40 unrewarded stimulations with 1-hexanol or 2-octanone. Odor stimulations lasted 4 s and the intertrial interval was 1 min. Three complete imaging sessions were repeated 10, 40 and 70 min after the end of the exposure session. The two measurements of each odor within each session were used to test for reliability of signals and were further averaged during analysis.

### Imaging analysis

Image analysis was done using software written in IDL (Research systems, CO, USA) by Giovanni Galizia and Mathias Ditzen (routines can be requested from the authors). Each measurement consisted of a double sequence of 50 fluorescence images obtained at 340 nm and 380 nm excitation light ( $F_{i340}$ ,  $F_{i380}$ , where  $i$  is the number of the image from 1 to 50). For each pair of images  $F_i$  we calculated pixel-wise the ratio  $R_i = (F_{i340} \text{ nm}/F_{i380} \text{ nm}) \times 100$  and subtracted the background ratio  $R_b$ , obtained by averaging the  $R_i$  values 1 s immediately before the odor onset [ $R_b = 1/5 (R_{10} + \dots + R_{14})$ ]. Resulting values, shown in the figure as  $\Delta R$ , represent the change from the reference window and are proportional to the changes in the intracellular calcium concentration. Quantitative analysis of odor-induced activity patterns was based on calcium signals in identified glomeruli. For this aim, glomeruli were identified on the basis of their morphology and relative position using the digital atlas of the honey bee AL as a reference (Galizia *et al.*, 1999). The visualisation of glomeruli was achieved by observing the raw fluorescence images obtained at 380 nm excitation light, and we additionally used software written by Mathias Ditzen that allows a clear view of glomerular shape and position. The software calculates images representing the degree of correlation between neighboring pixels. As glomeruli

respond as functional units, pixels stemming from the same glomerulus are highly correlated over time. In contrast, pixels from different glomeruli are uncorrelated. This provides images in which glomeruli are visible and clearly separated by contrasting boundaries. Figure 1A shows examples of raw and correlation images used for glomeruli identification. Eighteen glomeruli could be unequivocally identified across all animals and thus were used for the present analysis. All glomeruli are located in the dorsorostral side of the AL. We examined activity in glomeruli 17, 23, 24, 25, 28, 29, 33, 35, 36, 37, 38, 42, 43, 47, 48, 49 and 52, which belong to tract 1 from the antennal nerve, and glomerulus 45 from tract 3, according to the nomenclature previously established (Flanagan & Mercer, 1989; Galizia *et al.*, 1999). Glomerular activation was calculated by averaging activity in a square area of  $9 \times 9$  pixels that correspond to  $23.4 \times 23.4 \mu\text{m}$  and fits well within the boundaries of the glomeruli. Glomerular activity in the present study refers to activity of the uniglomerular PNs that innervate the selected glomeruli.

#### *Principal component analysis (PCA)*

Odor-induced activity patterns were characterised in the present study by measuring calcium signals in 18 identified glomeruli of the dorsal side of the AL. Therefore, each data point, i.e. each odor at each time point, is described by an 18-dimensional vector. We performed PCA (SPSS Inc.) to ease visualisation of the different activity patterns evoked by the three odors and also to show evolution of the patterns across time. The data set was reorganised as a single 2-D matrix composed of the three odors and all time points (frames) between 600 ms before odor onset and 2000 ms after odor offset as rows and 18 glomeruli as columns (example of a data point: 1-hexanol at 500 ms: glom17, glom23,...,glom52). This matrix was subjected to PCA and varimax rotation. The two-first principal components (PCs) explain 92% of variance in this example and clearly separate 1-hexanol, 2-octanone and the mixture. The data set of all 1-hexanol-exposed bees and all 2-octanone-exposed bees were correspondingly averaged to get two 'average bees' (see Methods in Fernandez *et al.*, 2009), the 1-hexanol bee and the 2-octanone bee, respectively. Each of the two average bees have data points that corresponded to the three odors at each time point of the measurement and at four sessions (before exposure and 10, 40 and 70 min after exposure). The data sets corresponding to the average bees were organised in a 2-D matrix, configured with each data point (odor/session/frame) as rows and 18 glomeruli as columns (example of one data point: 1-hexanol/10-min session/at 500 ms: glom 17; glom 23; ...; glom 52). The matrix was subjected to PCA and varimax rotation to reduce the 18 dimensions. The first PCs explain 97 and 95% of variance in the groups of bees exposed to 2-octanone and 1-hexanol respectively. Note that PCA performed on data from the average bees is used only for visualisation of the effect, while analysis and conclusions are strictly based on correlation analysis as explained in the next section.

#### *Pattern similarity assessment*

Odor-elicited patterns are represented as vectors with 18 elements and each element constitutes the glomerular activity averaged during 1 s of odor stimulation. Euclidean distances or correlation coefficients are normally valid parameters used to evaluate similarity between patterns. However, the accuracy of the two parameters as predictors of perceptual similarity between two odors might change depending on features of the odors that are to be compared. In a preliminary analysis we compared the outcomes of the two parameters for the three possible comparisons, i.e. 1-hexanol vs. 2-octanone, 1-hexanol vs. mixture

and 2-octanone vs. mixture. For the odors, concentrations and mixture compositions used in the present work, Pearson's correlation coefficient was a better predictor of the perceptual similarity than the Euclidean distances. Thus, throughout this study we used the Pearson correlation coefficient as the measure of similarity between the activity patterns evoked by two odors in the same animal and during the same session. In order to analyse whether the unrewarded exposure session biased the representation of the mixture towards or away from the representation of the components, we calculated the correlation coefficients between the mixture and the pure components for each bee and each session. Subsequently, the correlation values were categorised according to the odor used in the exposure session. Statistical analysis was based on a two-way repeated-measures ANOVA and contrasts between all post-exposure sessions and the pre-exposure session. For ANOVA, correlation values were grouped as exposed mixture or as novel mixture. Sessions were considered as repeated factors for statistical analysis. No significant difference was found between sessions, either for the exposed or the novel odors as separate factors. However, the interaction term and interaction contrasts between the pre-exposure session and the post-exposure sessions were statistically significant.

#### *Electroantennogram (EAG)*

EAG recordings were performed to test for a possible decrement in olfactory input after exposure training. Honey bees were caught, restrained in Plexiglas holders and fed following the same procedure described for the imaging experiments. The head was fixed to the holder with wax and a  $25 \mu\text{m}$  uninsulated silver wire was inserted into the right eye and used as ground electrode during recordings. The position of the antennae was fixed with eicosane and the tip of the left antenna was cleanly cut. A glass microelectrode filled with a 0.1 M KCl solution mounted on a WPI electrode adapter was inserted through the open tip of the antenna. The EAG signal was fed into a DAM50 Bio-Amplifier (WPI). The output was digitised with an analog-digital converter (Lab-Trax 4; WPI) and recorded for offline data analysis (Data-Trax 2; WPI). Stimulation conditions, odor concentration, stimulus duration and odor sequence were identical to those used for imaging experiments. Only two recording sessions were performed and they corresponded to the first and second sessions of the imaging experiments. These sessions were separated by 60 min. The first session finished 10 min before starting the 40-min exposure session and the second recording session started 10 min after the end of the exposure session. The exposure session that followed was identical to the exposure session for the imaging experiment. Amplitude of odor-induced signals was calculated by subtracting the potential recorded before odor onset. All of the analyses were based on the average of two measurements per odor and per session. Statistical analysis was based on two-way repeated-measures ANOVA with odor as an independent factor (novel odor/exposed odor/mixture) and sessions as a repeated factor.

#### *Behavior*

Honey bees were exposed to an odor and later conditioned to a mixture that contained that odor in order to measure whether exposure affects learning performance to the mixture. Animals were captured, restrained and fed following the same procedures used in imaging and EAG experiments. One day after capture, animals were divided into three groups. Two groups underwent an exposure session identical to the exposure session used in imaging experiments. The exposure session lasted 40 min and consisted of  $40 \times 4$  s unrewarded stimulations with 1-hexanol or 2-octanone. A blank group

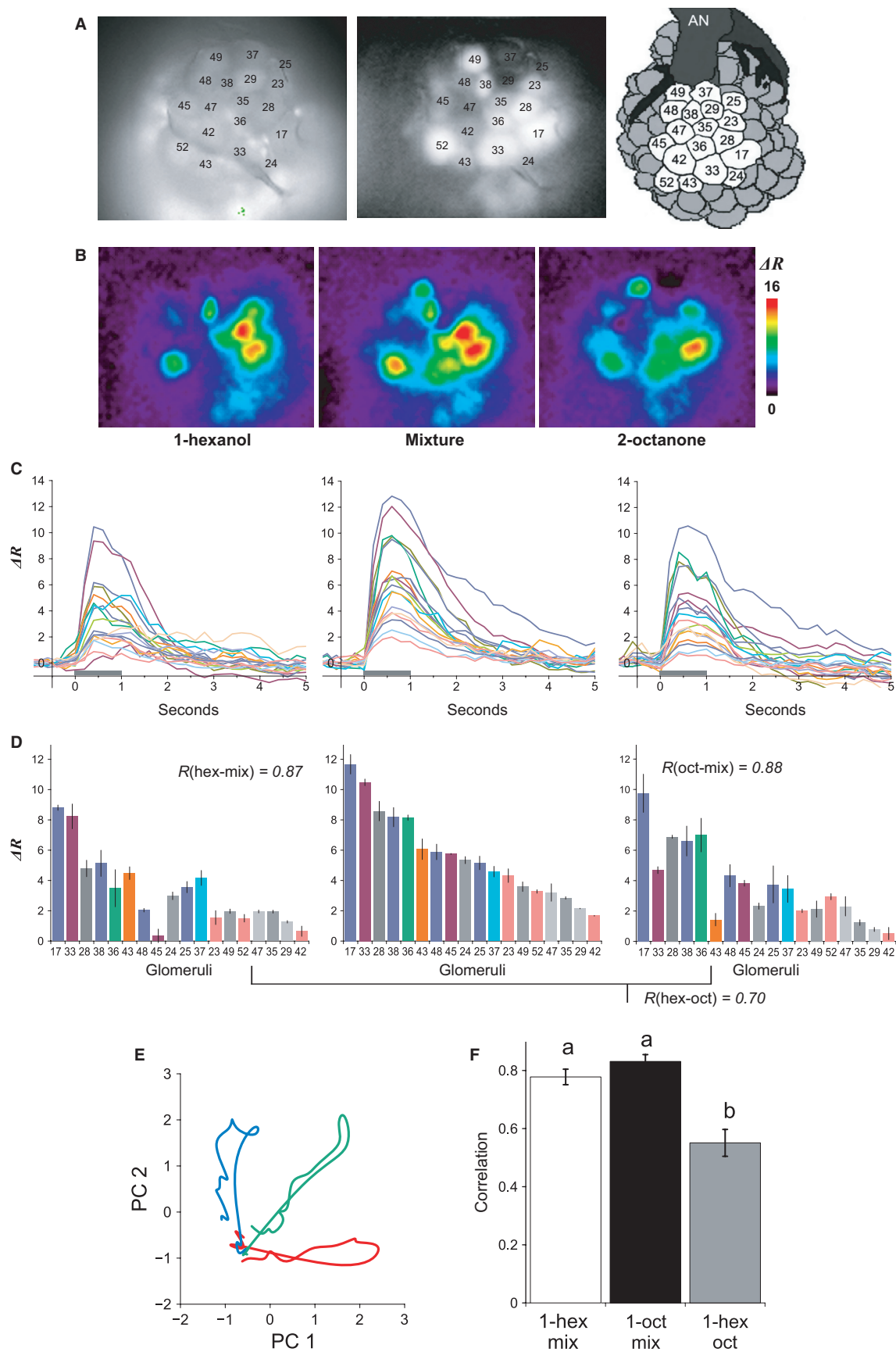


FIG. 1. Calcium imaging of projection neurons in the honey bee AL. (A) View of the AL after staining the PNs. The picture shows the dorsal surface including 18 identified glomeruli (Galizia *et al.*, 1999) used for the imaging analyses. (Left) Basal fluorescence images, obtained with 380-nm excitation light and LP510 emission filter, allowed identification of glomeruli according to size, shape and position by comparison with the published honey bee AL atlas (Flanagan & Mercer, 1989; Galizia *et al.*, 1999). Basal fluorescence images were also used for verification of homogeneous staining in all glomeruli used for analysis. (Center) Correlation images (see Materials and Methods) clearly define boundaries between glomeruli and thus were used as an additional tool to verify glomeruli identification. Darker glomeruli do not indicate lack of staining (controlled for from the images such as the one in the left panel); these glomeruli were not activated by the odors and consequently produce a low correlation value with neighboring pixels. (Right) Schema of the dorsal surface on the honey bee AL showing 18 glomeruli used in our analyses (AN, antennal nerve). (B) Color-coded (see scale) changes in calcium levels averaged between 400 and 800 ms after odor onset. The figures show distinct but slightly overlapping spatial activity patterns for each of the three odors. (C) Glomerular activity over time to show spatiotemporal activity patterns. The same line color across figures represents the change in ratio over 6 s (1 s before stimulation through 5 s after) in a single identified glomerulus for each of the three odors. (D) Calcium responses for each of the 18 glomeruli averaged over 1 s of stimulation ordered from the highest response to the lowest for the mixture (middle figure). The same ordering was maintained for 1-hexanol (left) and 2-octanone (right) to emphasise changes in activity in each glomerulus for each of the odors compared to the mixture. Error bars represent SD of two measurements. *R*-values in D refer to the Pearson correlation coefficients used to compare pairs of odor patterns within animal and within session. (E) PCA (see Materials and Methods) used to show the evolution of the activity patterns over 200-ms time steps during odor stimulation in one animal (Galan *et al.*, 2006; Fernandez *et al.*, 2009) for 1-hexanol (blue), the mixture (green) and 2-octanone (red). With the onset of odor stimulation the transients for the pure odors project along each PC axis and reach maximal separation between 400 and 600 ms (Fernandez *et al.*, 2009). After odor termination the transients loop back and return to origin. (F) Mean  $\pm$  SE of the correlation coefficients indicated in D, for 17 animals prior to any treatment. The correlations between the pure components and the mixture are significantly higher than the correlation between the pure odorants; different letters on tops of the bars indicate significant differences at  $P < 0.01$ .

was manipulated in the same way but received only clean air during the whole exposure session. Fifteen minutes after the end of the exposure session all groups were subjected to olfactory conditioning of the proboscis extension reflex (Bitterman *et al.*, 1983), during which all animals were identically conditioned to a 1 : 1 mixture of 1-hexanol and 2-octanone over three trials. During conditioning, animals received a sucrose reward 3 s after odor onset. Reward consisted of first touching the antennae with a 2.0 M sucrose–water solution, which elicited proboscis extension, and then feeding with

0.4  $\mu$ L of the solution. The intertrial interval was 10 min. Fifteen minutes after the end of the conditioning session, the conditioned response was assessed in a test session using 1-hexanol or 2-octanone. Each animal was tested only once. Proboscis extension was recorded as a binary variable (proboscis extension or not) during the training and test trials. Extension of the proboscis beyond the virtual line between the open mandibles during odor presentation was effectively counted as proboscis extension. On acquisition trials, the response was determined for each subject as positive if the subject

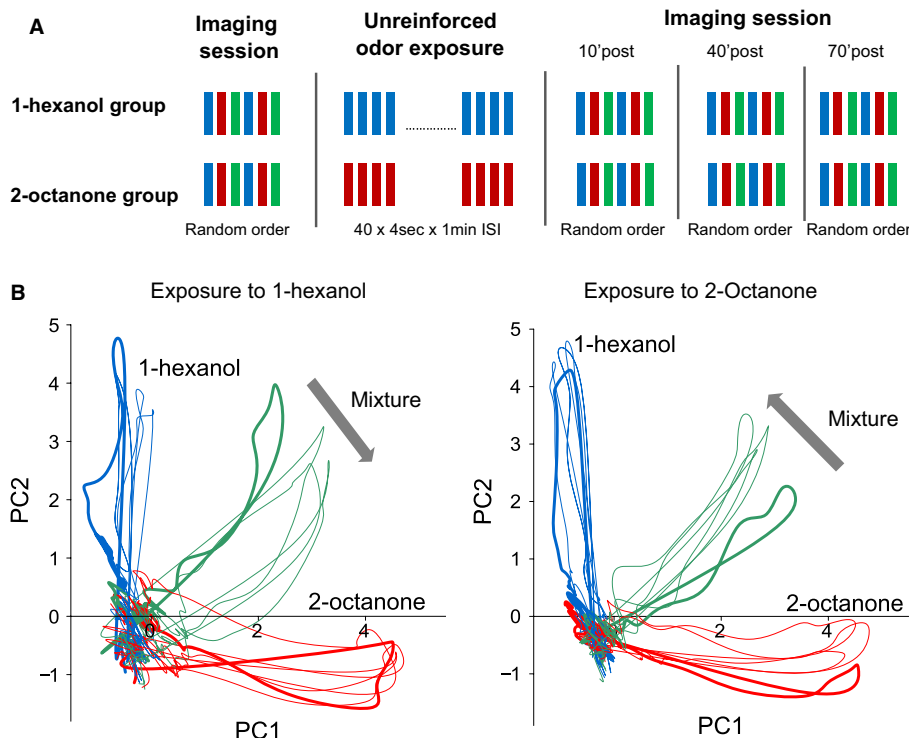


FIG. 2. Effect of odor exposure on odor-induced spatiotemporal activity in the AL. (A) Experimental protocol: each imaging session includes two stimulations each with 1-hexanol, 2-octanone and the mixture (1 : 1) distributed in random order and separated by a 1-min interstimulus interval (ISI). The exposure consisted of  $40 \times 4$  s presentations of either 1-hexanol or 2-octanone separated by a 1-min ISI. The exposure session started 5 min after the end of the first imaging session. Odor representations were measured again in the second, third and fourth imaging session performed 10, 40 and 70 min after the end of the exposure, respectively. (B) Odor-elicited responses from 18 glomeruli are represented using PCA. The animals exposed to 1-hexanol ( $n = 8$ ) and to 2-octanone ( $n = 9$ ) were separately averaged to obtain two average bees with 18 glomeruli each (see Materials and Methods; also Fernandez *et al.*, 2009). The 18 dimensions used to describe odor transients were reduced to its first two PCs (95 and 97% of the total variance respectively). Bold lines indicate the first imaging session, which was done before the exposure session. Thin lines belong to the second, third and fourth imaging sessions performed after exposure. We used PCA for visualisation only. Statistical analyses as well as conclusions are based on the absolute correlation values presented in Fig. 3.

extended its proboscis during odor stimulation and before the unconditioned stimulus presentation. These data are plotted as the percentage of subjects that responded to the mixture on each trial during training or to the single odors during test trials.

### Odor stimulation

Odors used for stimulation were the aliphatic alcohol 1-hexanol and the ketone 2-octanone (98%; both TCI America, Portland, OR, USA), alone or combined in binary mixtures 1 : 1. Odors were diluted from purity 1/100 or 1/10 in mineral oil (M-8410; Sigma-Aldrich) for imaging or behavior experiments. The output of the odor delivery device, for both behavioral and imaging experiments, was positioned 2 cm away from the animal's head and the air stream was aimed toward the antennae. During the periods without odor stimulation a continuous charcoal-filtered air stream (25 mL/s) ventilated airspace around the antennae. A constant exhaust removed odors from the arena. The odor cartridges consisted of a 1 mL glass syringe containing a filter paper strip (0.5 × 8 cm) loaded with either 5 µL 1-hexanol solution + 5 µL mineral oil, 5 µL 2-octanone solution + 5 µL mineral oil or 5 µL 1-hexanol solution + 5 µL 2-octanone solution. Three-way valves (LFAA1200118H; The LEE Company, Essex, CT, USA) controlled the onset of the airflow through the odor cartridge. When the valve was open, the air inside the cartridges was pushed into the continuous air stream in a mixing chamber 2 cm before the output of the odor delivery device. During behavior experiments, opening and closing of the valves was triggered by a programmable controller (Automation-Direct) and the odor duration was 4 s. During imaging experiments, the opening of the valve was synchronised with the optical recordings by the imaging acquisition software TILLVISION (TILL Photonics). In an earlier study (Fernandez *et al.*, 2009) we found that odor durations of 600 ms or longer leads to odor recognition independent of the duration of stimulations. This allowed us to reduce the odor stimulation during the imaging sessions to only 1 s and shorten the whole duration of the imaging protocol. This shortening is important as the UV light (340 and 380 nm) needed for the calcium imaging recordings is targeted to the animals brain and long exposures lead to cell damage by phototoxicity. The odor delivery device had eight independent and identical channels, each of them composed of a valve attached to an odor cartridge. Between experiments, odors were rotated to balance possible differences between channels.

### Conductance-based model

The model network consists of 20 PNs and 20 local neurons (LN)s wired according to the generative model shown in Fig. 6A. The basic structure of the model (Bazhenov *et al.*, 2001) was used with some modifications to better account for the calcium current. The LN>s receive input from olfactory receptor neurons (ORNs), other LN>s and PNs (Distler *et al.*, 1998; Wilson *et al.*, 2004). The PNs integrate the incoming ORN and LN activity as well as the sparse input from other PNs. The membrane potential  $V_{PN}$  of each PN and LN is modeled by the differential equation

$$C_m \frac{dV_{PN/LN}}{dt} = -g \times (V_{PN/LN} - E) - I_{Na} - I_K - I_{Ca} - I_{KCa} - I_{syn} - I_{stim}$$

where the reversal potential was  $E = 55$  mV, the membrane capacitance was  $C_m = 0.1$  nF and the membrane conductance was  $g = 0.04$  µS. Note that LN>s in the honeybee are spiking neurons, in contrast to the LN>s of the locust AL.

### Intrinsic currents

$I_{Na}$  and  $I_K$  are described by  $I_X = g_X n^X h^M (V_{PN/LN} - E_X)$  with the gating variables  $n$  and  $h$  evolving according to  $\frac{dn}{dt} = (n_\infty(V_{PN/LN}) - n)/\tau_n(V_{PN/LN})$  and  $\frac{dh}{dt} = (h_\infty(V_{PN/LN}) - h)/\tau_h(V_{PN/LN})$ , both within the interval [0,1].

For the fast sodium current  $I_{Na}$ , the parameters were  $g_{Na} = 5$  µS,  $N = 3$ ,  $M = 1$ ,  $E_{Na} = 50$  mV,  $\tau_n = 3/(\alpha_n(V_{PN/LN}) + \beta_n(V_{PN/LN}))$ ,  $n_\infty = \alpha_n(V_{PN/LN})/(\alpha_n(V_{PN/LN}) + \beta_n(V_{PN/LN}))$ ,  $\tau_h = 3/(\alpha_h(V_{PN/LN}) + \beta_h(V_{PN/LN}))$  and  $h_\infty = \alpha_h(V_{PN/LN})/(\alpha_h(V_{PN/LN}) + \beta_h(V_{PN/LN}))$ , where  $\alpha_n(V_{PN/LN}) = -0.32 \cdot (V_{PN/LN} + 42)/(e^{-0.25 \cdot (42 + V_{PN/LN})} - 1)$ ,  $\beta_n(V_{PN/LN}) = 0.28 \cdot (V_{PN/LN} + 15)/(e^{0.2 \cdot (V_{PN/LN} + 15)} - 1)$ ,  $\alpha_h(V_{PN/LN}) = 0.128 \cdot e^{-(38 + V_{PN/LN})/18}$  and  $\beta_h(V_{PN/LN}) = 4/(e^{-0.2 \cdot (15 + V_{PN/LN})} + 1)$ .

For the fast potassium current  $I_K$ , the parameters were  $g_K = 1$  µS,  $N = 4$ ,  $M = 0$ ,  $E_K = -95$  mV,  $\tau_n = 3/(\alpha_n(V_{PN/LN}) + \beta_n(V_{PN/LN}))$  and  $n_\infty = \alpha_n(V_{PN/LN})/(\alpha_n(V_{PN/LN}) + \beta_n(V_{PN/LN}))$ , where  $\alpha_n(V_{PN/LN}) = -0.32 \cdot (V_{PN/LN} + 30)/(e^{-0.2 \cdot (V_{PN/LN} + 30)} - 1)$  and  $\beta_n(V_{PN/LN}) = 0.5 \cdot e^{-(V_{PN/LN} + 35)/40}$ . The intrinsic calcium current is described using the Goldman–Hodgkin–Katz formalism due to the large differences in calcium concentration between inside and outside the cell. If we assume that the calcium differences are always large we can write  $I_{Ca} = 0.2n^3hV_{PN/LN}/(1 - e^{2V_{PN/LN}/24.42})$  (Huerta *et al.*, 2000; Szűcs *et al.*, 2009) where the gating variables  $n$  and  $h$  satisfy the differential equations above with the parameters  $\tau_h = 20 - 19.9/(1 + e^{(V_{PN/LN} - 40.1)/8})$ ,  $n_\infty = 1/(1 + e^{(-V_{PN/LN} - 27.1)/7.18})$ ,  $\tau_h = 30 + 100/(1 + e^{(V_{PN/LN} + 50.1)/5})$  and  $h_\infty = 1/(1 + e^{(V_{PN/LN} + 27)/3.5})$ .

The calcium-dependent potassium current was modeled by  $I_{KCa} = 0.15(V_{PN/LN} + 95)([Ca]^4/([Ca]^4 + K_{Ca}^4))$ , where  $K_{Ca} = 0.5$  µM. Here, [Ca] denotes the calcium concentration, which is described by a first-order kinetic equation as follows:  $d[Ca]/dt = 0.001(4I_{Ca} - 0.42[Ca] + 0.1)$ . To stay consistent with the experimental calcium measurements, the read-out from the PN was made through the calcium concentration.

### Synaptic currents

The stimulus current  $I_{stim}$  to  $i$ -th PN was considered to be a current pulse of the ORN to which the PN is attached (as shown in Fig. 6A). The synaptic current into the  $i$ -th PN was the sum of currents from adjacent inhibitory LN>s. For each adjacent LN  $j$ , the synaptic current was described by  $I_{syn}^j = g_i^j(V_{PN}^i + 80)/(1 + e^{(0.5 - V_{LN}^j)/7})$ , where  $g_i^j$  is the conductance associated with the synapse from the  $j$ -th LN to the current ( $i$ -th) PN, and  $V_{LN}^j$  is the membrane potential of the  $j$ -th LN. For each excitatory synapse (arriving from the  $j$ -th PN), the synaptic current component was described by  $I_{syn}^j = g_i^j r(V + 70\text{ mV})$ , where  $g_i^j$  denotes the conductance of the synapse (now arriving from  $j$ -th PN) and  $r$  is the bound receptor state, which is subject to the dynamics  $dr/dt = \alpha \cdot [T](1 - r) - \beta \cdot r$  as proposed in Destexhe *et al.* (1994). Here,  $[T]$  denotes the transmitter concentration in the form of a pulse, that is,  $[T] = 1$  µM within the first 2 s following a spike in the presynaptic PN, and  $[T] = 0$  otherwise. The rise and decay constants  $\alpha$  and  $\beta$  were selected as  $10^{-4}/\text{ms}/\mu\text{M}$  and  $2 \times 10^{-4}/\text{ms}/\mu\text{M}$ , respectively.

### Firing-rate model

A firing-rate model was used to concentrate on the role of the synaptic transmission without taking into effect the intrinsic dynamics of the neurons. The rate model was used as it allows more effective evaluation of which aspects of the connectivity and its plasticity are relevant to explain a given phenomenon. As rate model we use the

well known Wilson–Cowan rate model (Wilson & Cowan, 1972). This simple model consists of  $N_{\text{PN}}$  excitatory PNs and  $N_{\text{LN}}$  inhibitory LNs, units whose activities evolve according to

$$\frac{dx_i}{dt} = \Theta \left( - \sum_{j=1}^{N_{\text{LN}}} w_{ij}^{\text{EI}} \cdot y_j + E_i(S) \right), \quad i = 1, \dots, N_{\text{PN}},$$

$$\frac{dy_i}{dt} = \Theta \left( \sum_{j=1}^{N_{\text{PN}}} w_{ij}^{\text{IE}} \cdot x_j - \sum_{j=1}^{N_{\text{LN}}} w_{ij}^{\text{II}} \cdot y_j + I_i(S) \right), \quad i = 1, \dots, N_{\text{LN}},$$

respectively. Here  $\Theta(\cdot)$  denotes the piecewise linear activation function. The connectivity and conductance values were generated by a Bernoulli process, which assigned to each element of the matrices  $\mathbf{W}^{\text{EI}}$  the value 1.0 with probability 0.5 independently, or 0 otherwise. The second connectivity matrix  $\mathbf{W}^{\text{IE}}$  was generated in the same way for the conductance value 0.5.  $\mathbf{W}^{\text{II}}$  was set with probability of 0.4 and conductance of 0.5. The stimulus was injected into the network through the PNs with  $E_i(S)$  and LNs using the term  $I_i(S)$ . This function generates an arbitrary pulse value of 5 for the pure odor A and for the pure odor B, reaching a different subset of PNs for different odors (note that the arbitrary value does not change the results). It is set to 0 when there is no odor present at the input.

### Synaptic plasticity

The firing-rate model and the conductance-based model were used to test three different hypotheses of synaptic plasticity that may account for the changes observed in the representation of the mixtures: they were plasticity in synapses: (i) from LNs to PNs; (ii) from PNs to LNs; and (ii) from LNs to LNs. If the observed changes could not be reproduced using simple models and basic plasticity rules, then the mechanisms of synaptic plasticity that we propose may not be sufficiently general. In this regard, note that the model's dynamics are driven by intrinsic elements of the AL network and direct inputs from the ORNs. The model does not consider feedback from other brain regions (Rybäk & Menzel, 1993; Kirschner *et al.*, 2006; Hu *et al.*, 2010) and it does not consider modulatory inputs (Hammer, 1997) that are needed for associative learning.

## Results

### *Odor exposure changed competition between components in a mixture*

Our previous analyses of nonassociative olfactory conditioning in honey bees have shown that 20 or more presentations of an odor without reinforcement, at 30 s or 5 min intervals, delays subsequent learning of an association of that odor with sucrose reward (Chandra *et al.*, 2010). We set out to evaluate whether the neural basis for this nonassociative conditioning, or at least a component of it, might reside in the first synaptic relay for olfaction in the brain, the AL. We employed a well-established method for using a calcium indicator to backfill axons of the PNs that innervate identified glomeruli on the dorsal surface in the AL (Fig. 1A; also Sachse & Galizia, 2002). This method has revealed robust odor-specific spatiotemporal activity patterns that reflect differential activation of PNs during and shortly after odor stimulation (Fig. 1B–E; also Galan *et al.*, 2006; Fernandez *et al.*, 2009). These ‘transients’ define a sequence of activity patterns

across glomeruli of the AL. The activation of glomeruli changes from one time point to the next, and the identity of the odor can be defined by the identity of the activated glomeruli, their relative activation and the sequence of states in the transient. Mixing two pure odorants produces a graded change in activity that is proportional to the mixture (Fernandez *et al.*, 2009). Binary mixtures that are biased toward one component (e.g. 9 : 1 or 7 : 3) are statistically more similar to the dominant component. Furthermore, differentially reinforcing two mixtures increases the separation of the transients for those mixtures (Fernandez *et al.*, 2009), which indicates that associative plasticity influences odor representations in the AL.

We chose two odors (1-hexanol and 2-octanone) used in our previous analysis of plasticity in the AL (Fernandez *et al.*, 2009) because they elicit distinct but slightly overlapping activity patterns (Fig. 1B–D; also Sachse *et al.*, 1999). A 1 : 1 mixture elicits an activity pattern that is intermediate to the components. Using PCA to reduce the number of dimensions from 18 to 2, we plotted this activity over 200 ms time steps from shortly before odor presentation through several steps after termination of the stimulus (Fig. 1E shows transient patterns from a single animal). The pattern of activity through time produces a transient through this two dimensional space that projects out and begins to return before the odor is terminated (Fdez Galán *et al.*, 2004; Mazor & Laurent, 2005; Fernandez *et al.*, 2009). The Euclidian distance between corresponding time points across the transients reaches a maximum approximately 400–600 ms after odor onset (Fernandez *et al.*, 2009). From background activity near the origin, the transients for the two pure odors run approximately parallel to each axis whereas the transient for the mixture projects at an angle intermediate to the other transients (Fig. 1E and Fernandez *et al.*, 2009). The similarities between the patterns elicited by the pure odorants and the mixture are reflected in the Pearson correlation values between the glomerular activity patterns (Fig. 1D and F). Each pure odorant is more similar to the mixture than the pure odorants are to each other. Figure 1F averages the correlation coefficient for the three odor pairs obtained for 17 animals (different letters indicate significant differences by LSD contrasts  $P < 0.01$  after significant ANOVA:  $F_{2,48} = 19.49, P < 0.0001$ ).

Our experiments included four identical imaging sessions (Fig. 2A). The first imaging session occurred prior to exposure treatment and was used to establish the AL response patterns prior to training. Then we presented animals with 40 unreinforced exposures to an odorant. This treatment is sufficient to decrease the probability that the odor will elicit a conditioned response when associated with reinforcement (Chandra *et al.*, 2010). The exposure treatment was followed by three additional test series performed 10, 40 and 70 min after the end of the exposure treatment. We could then compare the responses among the pure odorants and the mixture during each of the four test sessions.

Unreinforced exposure changed the way the AL network processed odors. The most dramatic effect was a shift in the transient for the mixture (Fig. 2B). After exposure to a pure odor, the transient for the mixture shifted away from that odor and toward the pure odor that had not been exposed. The effect was the same for exposure to 1-hexanol (left panel) and 2-octanone (right panel).

This noticeable shift in the trajectory of the transients was reflected in the change in the correlation between each pure odor and the mixture. Figure 3A and B show the actual correlation values between pure odors and the mixture before (bold diamonds) and after (small diamonds) exposure for each animal. The correlation between a pure odor and the mixture is variable from animal to animal before exposure treatment. However, after exposure the response to the mixture became more correlated to the novel (non-

exposed) odor in 12 of 17 animals (Fig. 3A). Furthermore, the mixture became less correlated to the exposed odor (Fig. 3B) in 13 of 17 animals. The mean change ( $\pm$  SE) across animals in the correlation between the mixture and the two odors (novel and exposed) is shown in Fig. 3C. At all three post-exposure test times the novel odor became more similar to the mixture and the exposed odor became less similar. Statistical analysis was based on the raw correlation values presented in Fig. 3A and B. For two-way ANOVA we considered Odor condition (novel or exposed) as one factor and Session as the second and repeated factor. No significant effect was found either for odor condition ( $F_{1,32} = 0.222$ , NS) or for session ( $F_{3,96} = 0.378$ , NS); however, the interaction term was highly significant ( $F_{3,96} = 6.351$ ,  $P = 0.001$ ). All interaction contrasts comparing pre-exposure measurements vs. post-exposure measurements were significant: pre vs. post 10 min ( $F_{1,32} = 5.075$ ,  $P = 0.04$ ); pre vs. post 40 min ( $F_{1,32} = 10.292$ ,  $P = 0.003$ ) and pre vs. post 70 min ( $F_{1,32} = 12.038$ ,  $P = 0.002$ ).

#### *The change in the mixture representation was not a consequence of sensory adaptation*

In order to evaluate whether the changes that we observe have arisen from adaptation of sensory receptors on the antennae, we performed the following additional analysis and experiments. First, we calculated the global AL response for each odor as the sum of the activity elicited in all glomeruli (Fig. 4A). The rationale behind this analysis is that if sensitivity to a mixture component is reduced as a consequence of sensory adaptation, then PN activity should reflect the input reduction as though a lower odor concentration had been presented (Sachse & Galizia, 2003). A reduction in signal because of sensory adaptation should therefore be pronounced for the odor used for unreinforced exposure. As no differences were found for 1-hexanol- or 2-octanone-exposed bees, the data for the exposed odor, novel odor and mixture were pooled. Figure 4A shows the global response in the AL across four sessions. The data were not normalised to avoid occlusion of changes between sessions. Instead, the data are shown as absolute values of the sum of calcium responses in all measured glomeruli. There was no detectable reduction in the global AL activity for the exposed odor that would arise from sensory adaptation. The statistical analysis based on two-way ANOVA with Odor as one factor and Session as the repeated factor showed a significant effect of odor ( $F_{2,63} = 6.6$ ,  $P < 0.01$ ). This significant result is based on significant differences among the activity elicited by the mixture vs. pure odors (Tukey HSD contrasts,  $P < 0.05$  in both cases) and not between pure odors ( $P = 0.98$ ). This stronger response to the mixture is consistent with the fact that the activity elicited by the mixture involves the sum of glomeruli activated independently by each pure odor, as has been previously shown using imaging techniques that reflect activity in sensory neurons (Joerges *et al.*, 1997; Deisig *et al.*, 2006) and in projection neurons (Deisig *et al.*, 2010). Differences among sessions were statistically significant (session factor,  $F_{3,189} = 5.02$ ,  $P < 0.01$ ). Tukey HSD contrasts showed significant differences between the first and the third, and between the first and the fourth sessions ( $P < 0.05$  in both cases). The increase in activity across sessions was independent of the odor and not consistent with sensory adaptation. Finally, the interaction term was not significant ( $F_{6,189} = 0.08$ ,  $P = 0.99$ ), revealing that the observed changes along sessions were independent of the treatment.

Second, we performed EAG measurements to directly measure summed afferent activity from sensory neurons into the AL. We per-

formed two recording sessions that corresponded to the first and second session of the imaging experiments (Fig. 4B). The first recording session finished 10 min before the exposure protocol. A group of five bees was exposed to 1-hexanol and a second group of five bees was exposed to 2-octanone. The second recording session was performed 10 min after the end of the exposure protocol. If sensory adaptation was responsible for the results reported in the previous sections then the adaptation should be clearly expressed during this session. As there was no difference between the two groups of bees, and the amplitude of EAG signals evoked by 1-hexanol and 2-octanone were similar, we regrouped the data from 1-hexanol- and 2-octanone-treated bees into novel, exposed or mixture odor, as we had in the previous experiments. No change was observed 10 min after the end of the exposure for any of the odors (mixture, novel or exposed odors; Fig. 4B). Statistical analysis based on two-way ANOVA with Odor as one factor and Session as repeated factor revealed no effect of the main factors or for the interaction; session factor ( $F_{1,27} = 0.52$ , NS); odor factor (novel, exposed or mixture,  $F_{2,27} = 3.18$ , NS) and interaction term ( $F_{2,27} = 0.43$ , NS). The tendency to a stronger response obtained by stimulation with the mixture (Fig. 4B) is consistent with more sensory neurons recruited under this condition.

Finally, the level of the response measured during the second session may have been the sum of two separate effects, one related to the odor exposure and the other related to the 60 min gap between sessions. Therefore as a control in a separate set of animals we measured the responses during both sessions without exposing the animals to any treatment during the 60 min interval (Fig. 4C). Two-way ANOVA with Odor (pure or mixture) as one factor and Session as repeated factor revealed no effect for either the main factors or the interaction term (odor,  $F_{1,13} = 1.01$ , NS; session,  $F_{1,13} = 0.14$ , NS; interaction term,  $F_{1,13} = 0.03$ , NS).

In summary, both the global activity and EAG experiments failed to provide evidence of reduced sensory input for the exposed odor that could provide an alternative account for the shift observed in the representation of the mixture after exposure.

#### *A novel odor more easily overshadowed an exposed odor*

The imaging data indicate that the mixture became perceptually more similar to the novel odor as a result of exposure. Therefore, a novel odor should be more capable of overshadowing a preexposed odor in a behavioral test. We tested this possibility using a proboscis extension response conditioning procedure for restrained honey bees (Fig. 5A; also Bitterman *et al.*, 1983). Three groups of bees underwent exposure protocols of 40 unreinforced presentations at 1-min interstimulus intervals, as in the exposure treatments used in the previous sections. One group was exposed to 1-hexanol, another group was exposed to 2-octanone and a third group was exposed to clean air as control. Most odors elicit proboscis extension response with a low probability on the first trial (approximately 10% of honey bees show a response prior to associative conditioning). The genesis of these spontaneous responses is still not well understood (Smith *et al.*, 2006) but this probability was low and equivalent across odors we selected and treatment groups in our study. Furthermore, these responses completely disappear after 40 preexposures (Chandra *et al.*, 2010). Therefore, we did not record proboscis extension response during the unreinforced exposure. We followed the unreinforced exposure with three conditioning trials during which the 1 : 1 mixture was reinforced with sucrose in a way that produces robust conditioned responding to the odor. Statistical analysis of performance during conditioning was based on two way repeated

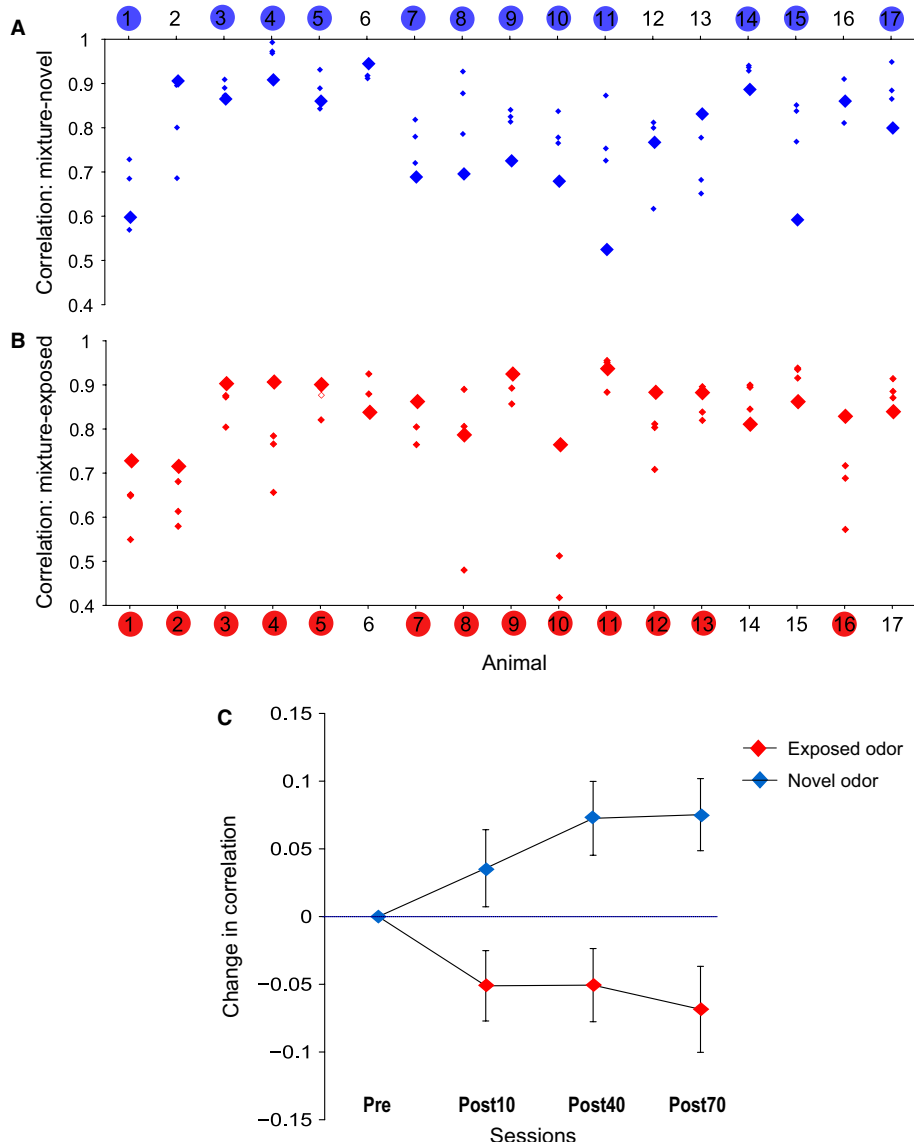


FIG. 3. Correlation coefficients between the mixture and the pure odors before and after exposure. (A) Absolute Pearson correlation coefficients between the activity patterns elicited by the novel odor (odor not used during exposure) and the mixture for each individual bee ( $n = 17$ ). Bold blue diamonds correspond to the correlation value before exposure. Small diamonds correspond to the correlation values after exposure. Numbers highlighted in blue indicate bees in which the average of the correlation from the three post-exposure sessions was higher than the correlation in the initial session. (B) Absolute Pearson correlation coefficients between the exposed odor and the mixture for each individual bee. Bold red diamonds correspond to the measurement performed before exposure and small diamonds to the measurements performed after exposure. Numbers highlighted in red indicate bees in which the average of the correlation values obtained in the three post-exposure sessions was lower than the correlation in the initial session. Statistical analysis was strictly based on raw correlation values as they are shown in figures A and B. Two-factor repeated-measures ANOVA: factor 1, novel or exposed odor, NS; factor 2, (repeated measurement) Session, NS; interaction,  $P = 0.001$ . (C) Data from A and B plotted as the net change in the correlation along the experiment. The panel shows the average and SEM of the difference between each post-exposure session and the session before exposure ( $n = 17$ ). The change in correlation was calculated within each bee by subtracting the correlation value obtained in the first test session from the values obtained in the post-exposure sessions.

measures ANOVA: “Trial” as the repeated factor showed a significant effect of training ( $F_{2,266} = 73$ ,  $P < 0.0001$ ), the “group” factor and the “interaction term” were not significant ( $F_{1,133} = 0.39$  and  $F_{4,266} = 0.7$ , respectively). Thus, honey bees in all three groups learned to respond equally well to the mixture (Fig. 5B).

Finally, after conditioning to the mixture we tested the response to each pure odor to evaluate the perceptual similarity of the mixture to the components. The responses to pure odors during the test depended on the exposure treatment. Honey bees responded equally to each of the pure odors after exposure to air (Fig. 5C, middle), which is the typical result for these odors in this protocol. This

response after mixture conditioning is typically lower than after conditioning to the pure odor (Smith, 1998), which indicates overshadowing. However, overshadowing is symmetric for animals that were pre-exposed to clean air. In contrast, exposure to odor prior to mixture conditioning caused overshadowing to become asymmetric. After exposure to 1-hexanol, the strongest response occurred to 2-octanone after mixture conditioning (Fig. 5C, left). In contrast, the strongest response occurred to 1-hexanol after exposure to 2-octanone (Fig. 5C, right). In Fig. 5D the data obtained during testing is shown and analysed independently of the odor identity and only based on the condition of the odor in the mixture, i.e. exposed odor,

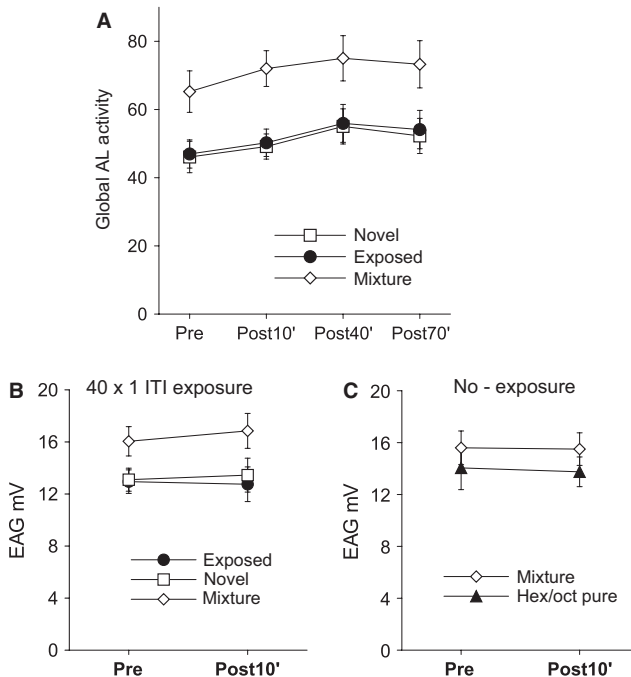


FIG. 4. Evaluation of sensory adaptation as a possible basis for the effect in the AL. (A) Global AL activity elicited by the exposed odor, the novel odor and the mixture along all sessions. The figure shows the sum of the calcium responses in the 18 measured glomeruli. No differences were found between 1-hexanol- and 2-octanone-exposed bees (data not shown). Data were therefore pooled for the exposed odor, novel odor or mixture and analysed along sessions. Statistical significance  $P < 0.01$  for both pure odors against the mixture and  $P < 0.01$  for first session against the third, and between fourth sessions for all odors; interaction not significant. The differences reported along sessions were not specific for the exposed odor. (B) EAG was performed for the mixture and the pure odors 10 min before and 10 min after the exposure protocol, coincident in time with the first and second session of the imaging experiments. Responses pre- vs. post- were not significantly different ( $n = 10$  bees). (C) A group of animals underwent two EAG sessions separated by 60 min, with no exposure protocol in-between, but coincident in time with the first and the second session of the imaging experiment. No change between the two sessions was observed ( $n = 5$  bees).

novel odor (for an odor accompanying an exposed odor) or any odor in case of the blank group.

Overall, the response to an odor after conditioning to a binary mixture containing that odor depended significantly on whether or not animals had been exposed to that odor without reinforcement (Fig. 5D, left column). Moreover, the response to a novel odor combined in a mixture with an exposed odor was enhanced (Fig. 5D, right column). The Kruskal–Wallis test showed statistical differences among responses elicited by the three odor conditions shown in Fig. 5D ( $F_{2,133} = 3.13$ ,  $P < 0.05$ ). Further statistical analysis using pairwise chi-square comparisons showed significant differences only between the novel and the exposed condition ( $P = 0.014$ ). The observation that learning scores for odors of the novel and the exposed condition were not statistically different from the learning scores for odors in the blank group but they were different from each other suggests a mechanism that biases learning of the novel and the exposed odor in opposite directions. In summary, this shift in the perceptually dominant component of the mixture toward the new odor was consistent with the imaging data.

#### *LN-to-PN connections were the most likely targets for nonassociative plasticity*

The imaging data and the resulting change in perception of the mixture imply an alteration in competitive interactions within the AL network. We used a well-established conductance-based model of transient dynamic coding in the insect AL (Bazhenov *et al.*, 2001) and a rate model (Huerta & Rabinovich, 2004) to explore which

synapses might be the most likely targets for future investigation. The network consisted of two clusters of 20 inhibitory LNs and 20 PNs (Fig. 6A). The odor inputs were modeled by injecting current to a particular set of PNs for odor A and another set of PNs for odor X. The level of overlap between the two PN groups was varied from 1 to 5 PNs in order to simulate odor pairs with different degrees of overlap. Each LN received inputs in a nonselective manner. In order to be consistent with the imaging data, the activity of PNs was monitored by the level of calcium set by the term  $I_{Ca}$  in the model (see Materials and Methods).

For consistency with the imaging experiments, the model employed a pretraining phase in which we used the initial network as it was generated by a Bernoulli process (Huerta & Rabinovich, 2004). The 20-dimensional PN (calcium) responses were recorded for pure odors A, X and the mixture. Plasticity was not applied at any synapse in this phase. We adopted the stimulation protocol used in the imaging experiments: the pure odor A, the pure odor X and the mixture (A + X) were applied sequentially to the network in a random order. These stimuli were encoded in a 20-dimensional binary vector with its entries denoting the presence or absence of the pure odors at the input. In each presentation, the network was stimulated with its corresponding PN activation group for 2 s and relaxed for the following 5 s until the onset of the next stimulation. This phase of the simulation allowed us to generate the 20-dimensional calcium trajectories representing the three types of stimuli and to form the PC space where we carried out the analysis.

In the training phase, the synaptic efficacy of a subset of LN-to-PN synapses was modified. The synapses affected in each presenta-

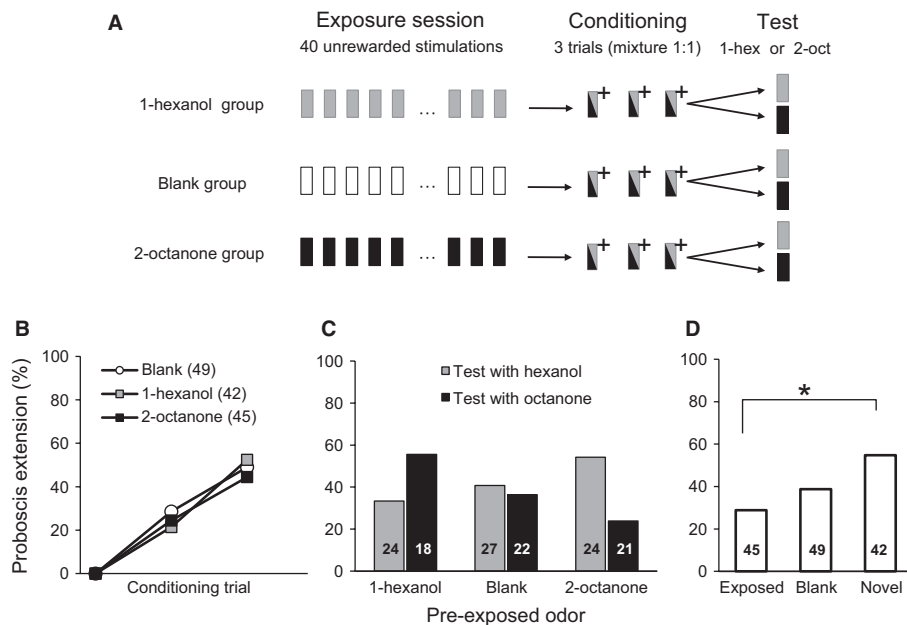


FIG. 5. Effect of repeated odor exposure on perception of an odor mixture. (A) Schema showing the experimental procedure. Exposure session: 40 unrewarded stimulations with 1-hexanol, 2-octanone or air (blank group); conditioning session: olfactory conditioning of the proboscis extension reflex (Bitterman *et al.*, 1983) using a 1 : 1 mixture (1-hexanol : 2-octanone); (+) indicates reinforcement with 0.4  $\mu$ L of 2 M sucrose paired with the mixture. Test session: conditioned response was tested with 1-hexanol or 2-octanone (animals were tested only once). Proboscis extension response during exposure protocol was not recorded, as these two odors do normally not elicit any response before conditioning. (B) Performance during conditioning showing percentage of animals extending the proboscis to the mixture during the three training trials. Results indicate % of response during the odor period and before reward. All groups were trained identically; they differed only in regard to treatment during the exposure session before training. No difference was found between the three groups but significant effects were found between trials for all groups. (C) Each of the three groups was split into two groups for testing with the pure components (1-hexanol or 2-octanone). Two-way ANOVA revealed a significant interaction between exposed odor (1-hexanol, 2-octanone or air) and test odor ( $F_{2,130} = 3.09$ ,  $P < 0.05$ ). Numbers in the bars indicate number of animals in each test condition in each exposure group. (D) Same data from C reorganised by exposed odor (1-hexanol and 2-octanone as test odors when animals had been exposed to 1-hexanol or 2-octanone, respectively), novel odor (1-hexanol and 2-octanone as test odors when animals had been exposed to 2-octanone or to 1-hexanol, respectively) and blank (1-hexanol and 2-octanone as test odors after exposure to air). \* $P < 0.05$  between exposed and novel odors.

tion were determined based on the instantaneous network activity. They were potentiated according to the following Hebbian learning rule: increase the conductance associated with all synapses where both the presynaptic LNs and the postsynaptic PNs are active (i.e. spiking). This modification was applied to each qualified synapse incrementally for each presentation during the training phase. The increment to the  $i$ th selected synapse was set as 5% of the current conductance value at the onset of the presentation. The potentiation saturated at 150% of the initial conductance of the synapse. In this plasticity scheme, most PN activity saturates within the first 10 presentations of the training odor. Note, however, that the applied plasticity progressively reduces the total excitation across the LN population, which in turn may reduce the total inhibition to the PN population. Therefore, the training time required for the synaptic connections to reach the bound and stabilise may be longer. For that reason we have kept the network in the training phase for 20 presentations, although the changes in the affected synaptic conductances vanished well before the end of training presentations due to the imposed 150% limit. In the post-training phase we fixed the synaptic conductances in the network and tested the network once again in random order with the pure odors A and X and the binary mixture.

Figure 6C shows the projected calcium trajectories in each phase of the experiment and for both training odors. The thick loops correspond to the presentations of odor A, X and the mixture during the initial phase before training. In each graph, the three thin loops in blue and red color correspond to the three representations of pure A and pure X during training and in the post-training phase. The three

thin green loops show the trajectory for the mixture at the 5th and 15th training trial and at the post-training phase in the order indicated by the arrow. Notice that the initial trajectories for the mixture may look different and shifted from the middle of the PC space in both figures even though they represent the pretraining state of the same network. The different shapes are due to different runs on separate PCAs for visualisation of the shift provoked by treatment.

We simulated 100 random networks generated independently using the connectivity shown in Fig. 6A. The average increment in a LN-to-PN synapse modified by odor exposure over all tested networks was relatively large (0.0373  $\mu$ S). As in the imaging experiments (Fig. 3C), the correlation between the mixture and the odor that was not exposed increased across trials (Fig. 6B). Exposure to either odor shifted the response to the mixture toward the novel (not exposed) odor (Fig. 6C and D). The increase in the correlation between the mixture and the novel odor was measured along 100 samples placed uniformly on the respective loops.

A successful AL network is defined as one that demonstrates a significant increase in such correlation, namely a 10% increase with respect to pretraining correlation. The correlation between two distinct network responses was calculated as follows: first, for each PN, the single-channel time series for the two stimuli were recorded during the exposure period. Then, the cross-correlation between such pairs of signals is obtained. The maximum correlation value over a range of time-lags between the time series was extracted as a similarity measure between the pairs of recorded signals. Finally, the correlations obtained for each pair of individual PN responses in this

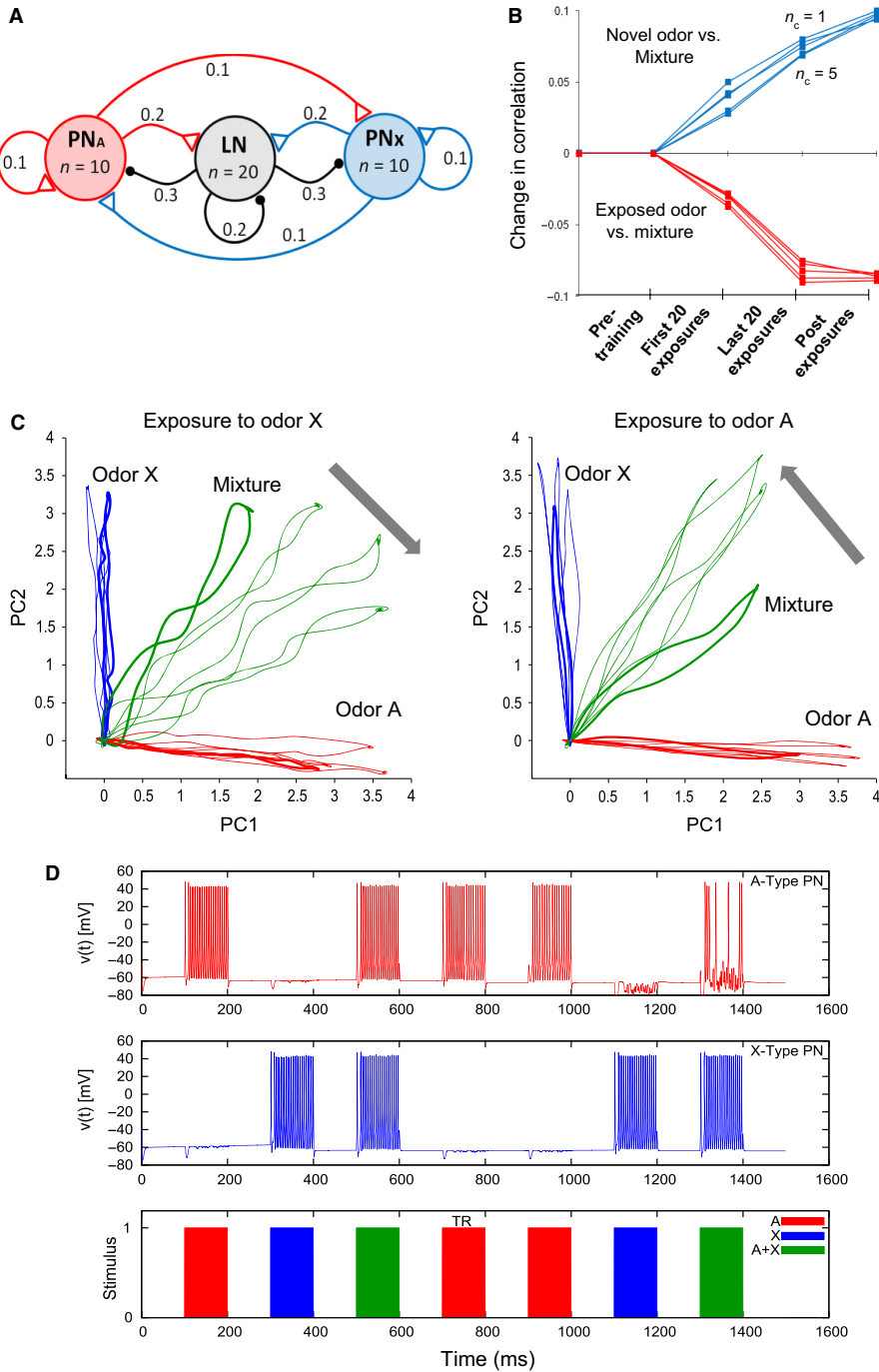


FIG. 6. Hebbian plasticity on LN-to-PN synapses predicted the imaging results. (A) Model of the AL topology used in the computational analyses. The network consists of 20 inhibitory local interneurons (LNs) and 20 projection neurons (PNs). This population is illustrated as three clusters in the figure. The connectivity within and between the clusters was determined randomly, based on the fixed probabilities indicated on the links. Connectivity probabilities related to individual neurons, i.e. each PN had a probability of 0.2 of connecting any neuron from the LN cluster; thus in our model each PN cluster made approximately 40 excitatory synapses onto LNs. The synaptic conductance for each type of connection was drawn from a normal distribution (by allowing no negative conductance). The mean  $\pm$  SD of these parameters were  $0.1 \pm 0.05 \mu\text{S}$  for within- and between-cluster synapses, and  $10 \pm 5 \mu\text{S}$  for the external stimulation. A particular odorant reached 10 PNs. Different degrees of overlap in the representation for A and X were evaluated by introducing from 1 to 5 common PNs (not shown in the schema). A pure odor was presented by injecting current into the set of PNs corresponding to odor A or odor X; the mixture was applied to the network by applying current in both A and X. (B) Change in correlation between the trajectories for the pure odors and the mixture before, during and after exposure training. The correlation was performed among ten samples (i.e. 10 loops on the 2-D PC plane) obtained for each category (i.e. odor A vs. mixture and odor X vs. mixture) and for increasing levels of overlap between odor A and odor X ranging from 1 to 5 common PNs. (C) The projections of the calcium trajectories of the PNs were obtained from the simulation of the computational model where each unit (PN or LN) was expressed by a conductance-based Hodgkin–Huxley-type single-compartment model. The training was performed on the same network for the two odor types. In line with the experimental protocol, the affected synaptic conductances were increased to 150% of their original values in 20 odor presentations during training. (D) The model's prediction of the membrane potential time traces for two arbitrary PNs, one from each response group. In this instance, the training was performed with odor A and all plasticity was encapsulated in the odor presentation labeled by TR.

way were added up and interpreted as the correlation between the two multidimensional PN responses. Out of 100 random realisations of the model, 98 of them demonstrated such an increase after the training phase, making them successful in reproducing the imaging data. The magnitude of potentiation during training trials and the saturation level regarding the synaptic conductances were tuned to maximise this success rate.

The total inhibition originating from LN activity into the PN population is the key quantity in this phenomenon (see Fig. 7 for an example of exposure to odor A). The total inhibition was always larger when the mixture (i.e. both odors A and X together) stimulated the network than when only odor A or X stimulated the network. By construction with the given parameters, the A-type PNs were initialised just above their firing thresholds. Upon training with odor A, the total inhibition onto A-type PNs was increased and most of these units turned silent when stimulated with the mixture. On the other hand, the bound introduced on the plasticity (i.e.  $1.5 \times$  the original conductance on the affected synapses) ensured that the total inhibition recruited by stimulus A after training was not enough to suppress responses in A-type PNs when stimulated with odor A alone.

We also used a rate model to investigate whether plasticity at specific synapses would be more effective in generating the changes we observed. In addition to the LN-to-PN plasticity, we tested PN-to-LN and LN-to-LN synaptic changes. Out of the 1000 train-test episodes performed on the sample networks for the rules LN-to-PN, PN-to-LN and LN-to-LN, 98.6, 76.3, and 32.4%, respectively, of the trials were successful. Based on these results, we included LN-to-PN and PN-to-LN synapses for further analysis with the conductance-based model and ruled out LN-to-LN. In order to test this prediction derived from the rate model we applied synaptic plasticity from the PN to LN in the conductance-based model, running 100 random realisations. We observed that 78 instances out of 100 random realisations were successful, and this is consistent with the success rates observed in the rate models. The LN-to-LN model was significantly less successful than LN-to-PN and PN-to-LN, to a probability value of  $P < 0.001$  with a power of 99.99%.

We also reproduced the phenomenon by using other hypothetical connections from the ORN into the AL. In particular, we tested the possibility that the LNs do not receive direct input from the ORNs such that they only get activated by the PNs (data not shown). The results also showed that the most effective connections to modulate information filtering were the LN-to-PN connections, which is consistent with the results previously described. It is remarkable that, regardless of the network design and stimulus input into the AL, the most effective connections for modulating the information filtering are LN-to-PN.

## Discussion

Our analyses are consistent with a model in which plasticity in the AL sets up a filter for processing odors (Smith, 1996; Smith *et al.*, 2006). It is now clear that associative and nonassociative mechanisms of plasticity are essential components of that filter (Faber *et al.*, 1999; Stopfer & Laurent, 1999; Sandoz *et al.*, 2003; Yu *et al.*, 2004; Sachse *et al.*, 2007; Denker *et al.*, 2010; Das *et al.*, 2011; Rath *et al.*, 2011). A major question that remains regards how these mechanisms interact to reshape the way the networks process sensory information. In the AL of the moth *Manduca sexta* (Daly *et al.*, 2004), different types of pairing of odor with sucrose reinforcement restructured the responses to odor in the AL network. Simply pairing odor with sucrose increased excitatory responses in

the AL, and presentation of odor alone decreased responses. Differential conditioning of one odor paired with sucrose and the other presented alone produced more complex switches between excitation and inhibition. Although it was clear from this work that both non-associative and associative plasticity influence the AL network, the function of this plasticity in terms of coding remained elusive. More recently, similar response changes in PNs of the AL after differential conditioning were reported for the honey bee (Fernandez *et al.*, 2009). This study went on to show that the changes served to increase the separation between the spatiotemporal response patterns for a reinforced vs. unreinforced odor, presumably making the odors perceptually more distinct (Sandoz *et al.*, 2003).

Here we have used calcium imaging to reveal that nonassociative mechanisms related to latent inhibition contribute to this separation by changing the competitive interactions between two different spatiotemporal activity patterns. The result is that a novel odor is more clearly represented in a binary mixture when it is combined with a previously unreinforced odor. We also show that these changes in the AL correlate to changes in perceptual properties of the mixture in behavioral experiments. The pair of odors used in the present work was selected because the odors have similar salience when separately used as a conditioned odor (Guerrieri *et al.*, 2005; Fernandez *et al.*, 2009), and neither perceptually dominates the other in behavioral or imaging experiments. As a 1 : 1 mixture produces a relatively graded change from either component, we felt that this condition was the best one with which to begin to look for plasticity-induced changes. Latent inhibition and overshadowing have been shown using several different odors (Smith, 1998; Chandra *et al.*, 2010), which indicates that our results will broadly apply to many odor pairs. Furthermore, our mathematical modeling also predicts that different degrees of overlap among the components should not affect the present conclusion. Nevertheless, the AL may have built-in or learned asymmetries in the way it processes different odors. Therefore, extension of our behavioral and imaging analyses to compare pairs of odors that have differing degrees of overlap or activation of glomeruli will be important.

The change in correlation among the pure odors and the mixture was very consistent across animals. The representation of the mixture became more similar to the novel odor and less similar to the exposed odor. Moreover, we showed that measuring only a fraction of the glomeruli in the AL, i.e. 18 out of 165, was sufficient to detect changes that correlated with the changes in the behavior. This perhaps surprising result might have two possible explanations. First, the glomeruli that are particularly relevant for this type of learning for these odors could have happened to be among the 18 glomeruli we targeted. That explanation seems less likely because we have not been able to identify single glomeruli that showed a statistically significant change after training, which is consistent with our previous report about plasticity in the AL (Fernandez *et al.*, 2009) as well as with related studies (Peele *et al.*, 2006; Rath *et al.*, 2011; but see Sandoz *et al.*, 2003; Yu *et al.*, 2004). Alternatively, and perhaps more likely, the plasticity driven by odor exposure may be small and distributed across many glomeruli. In Fernandez *et al.* (2009) and here we have shown that the change in the network is not dominated by one or two glomeruli. Instead, plasticity is reflected in the summation of small changes across many glomeruli. This interpretation seems consistent with the small but significant change reported after analyzing only 18 of the 165 glomeruli that conform the AL. If more glomeruli could be imaged the changes might be more obvious than the ones we report here. Furthermore, it is possible that plasticity affects different glomeruli in different animals such that the changes vanish when glomerular activity is

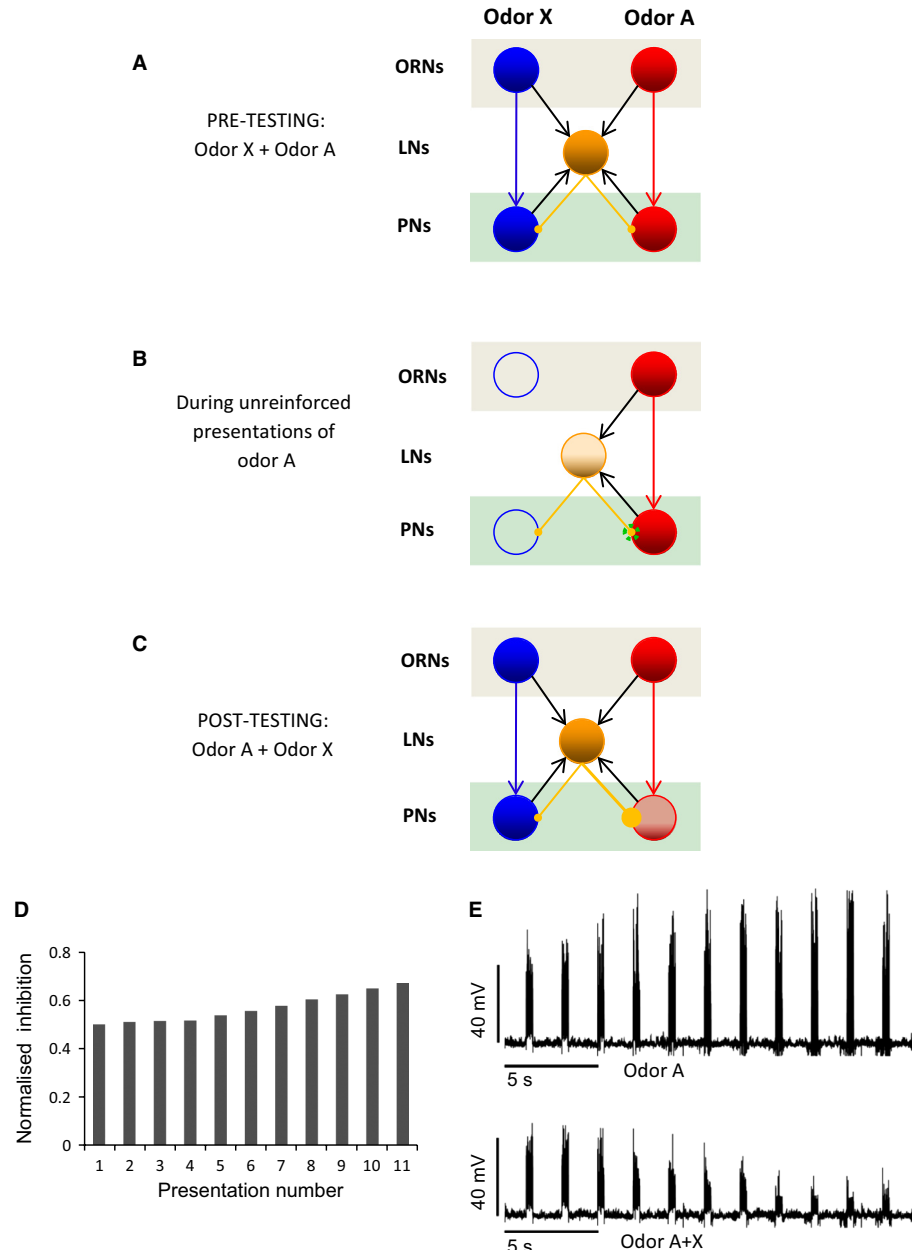


FIG. 7. Illustration of the simplest and most efficient mechanism for implementing filtering of uninformative odors in the AL. The schema indicates excitatory connections from ORNs to PNs and to LNs, excitatory connections from PNs to LNs and inhibitory connections from LNs to PNs. (A) Initially, lateral inhibition is weak and symmetric. The LN (yellow) receives input from both ORN clusters. As inhibitory connections are symmetric, the mixture induces a balanced representation of A and X across PNs. (B) Hebbian potentiation of inhibitory synapses during odor exposure. During training the connections from the LN to the PNs that are simultaneously active increase their synaptic strength. (C) the LN receives input from both ORN clusters and the inhibitory connection with PN-A was potentiated. When the odor mixture A + X is presented, the PNs responding to A become silent due to the increase in the overall inhibition arriving into those PNs as a result of training. As consequence, the blue (X) odor is more strongly represented in the pattern elicited by the mixture. In other words, odor A + X recruits a higher level of synaptic inhibition into group A than group X. (D) The fraction of total inhibition on the odor-A PN group vs. the total inhibition in the system after consecutive odor-A presentations in B. (E) Average membrane potential of the odor-A PN population for several presentations of that odor. The upper figure is the response when only odor-A is presented. The lower figure shows the diminishing response in the same A group during successive presentations of the A + X mixture.

averaged across bees. Variability across animals might be expected given that we used forager bees for the experiments, and each animal could have had its olfactory network shaped by different experiences in the field.

The changes we observed might be related to mechanisms of non-associative plasticity already described in the AL. Protein kinase A is important for nonassociative plasticity in the AL (Muller & Hilde-

brandt, 2002), and this could be an important mechanism underlying the plasticity at the circuit level that we describe. Also, unreinforced exposure to an odor can increase synchronisation among PNs (Stopfer & Laurent, 1999) or induce odor-specific changes in spontaneous background activity (Galan *et al.*, 2006). However, the latter effects last only a few minutes. In contrast, we show that exposure alters competitive interactions with other odors that lasts up to 70 min

and, behaviorally, latent inhibition lasts at least 24 h (Chandra *et al.*, 2010). More detailed analyses will be needed to reveal whether these forms of nonassociative modification of the AL are related, and will require a more detailed understanding of the neural mechanisms that underlie them.

As a first step toward investigating the possible underlying neural mechanisms, we have chosen to implement nonassociative plasticity in a well-developed model of the insect AL (Bazhenov *et al.*, 2001). Our modeling efforts performed both with realistic conductance models and with mean firing rate models replicated the experimental findings. We found that the most effective manner to filter out a repetitive unreinforced stimulus is by applying a Hebbian type of plasticity from the LNs onto the PNs. Even though other synaptic changes were also valid to some extent, the LN-to-PN connectivity changes were the most consistent in implementing filtering of frequent repetitive information. This result corresponds to a recent report of nonassociative modification of the fruit fly AL response to carbon dioxide, which occurs at least in part because of modification of LN-to-PN synapses (Sachse *et al.*, 2007). Moreover, odor-specific habituation in the fruit fly AL was recently mapped to these same synapses (Das *et al.*, 2011). Thus our model, which was inspired by behavioral and imaging studies we reported here in the honey bee, has been validated by empirical studies in the fruit fly that identified the same type of synapse.

Furthermore, our model has gone beyond earlier studies to suggest why plasticity specifically at these synapses is the most effective way to modify the circuit. The reason that LN-to-PN synapses are more effective is that there is a more direct and specific connection to the PN. When a PN and LN are coactivated only that synapse becomes modified (Fig. 7A–C). Modification of a PN-to-LN synapse would more often equally inhibit several PNs, including ones that are not involved in the response to odor. For example, modification of the red PN-to-LN connection in Fig. 7A would equally change the inhibition to the blue and red PNs. Therefore, plasticity from the PN into LNs was relatively less effective because this pathway represents second-order synapses onto the PN population. The second-order nature of the connections makes it more challenging to engineer the filtering mechanism by means of local or Hebbian type learning rules, although the filtering effect may arise for some favorable asymmetric initial set of network connections.

It is conceivable that the same result, in terms of both the AL activity and the behavioral conditioning, would arise if the response in activated ORNs were to decrease, for example through some form of adaptation or Hebbian decrease in the synaptic strength of the ORN-to-PN connection. However, we observed no evidence of change in PN activity after odor exposure. Furthermore, this may not be an adequate means to accomplish filtering. This kind of modification would more directly, and perhaps more significantly, diminish an animal's ability to process an odor when the meaning of that odor changes. Using the indirect route that we propose would at least allow the PN to be activated, which might turn out to be an important means for reversing the plasticity when necessary. We have not extensively tested this possible model yet, at least beyond what we present in Figs 2 and 5.

We did not find any indication of changes in the spatiotemporal representation of the exposed or the novel odor as a result of unreinforced odor exposure. The correlation coefficients between the exposed and the novel odor were the same before and after conditioning. Instead, the changes induced by training became evident only in the representation of the mixture. The computational model that we implemented was useful to define that this outcome is possible under certain levels of inhibition and specific plasticity rules.

The increased level of inhibition at LN to PN synapses after unreinforced exposure, together with the higher amount of inhibition recruited by the mixture, were sufficient to inhibit PNs of the exposed odor. Alternatively, the total amount of inhibition recruited by the exposed odor alone was insufficient to inhibit the PNs activated by the exposed odor. Therefore the exposed odor could still be processed when presented alone.

The filtering effect is very relevant in the context of information processing in the brain. Stimuli that occur frequently and without direct consequences have much less information than rare ones, and this may or may not have consequences (Shannon, 1948). We argue that the AL facilitates odor discrimination by reducing information that is not relevant via a Hebbian plasticity rule from the LNs to the PNs, which operates without reinforcement. It helps to reduce the importance of information that occurs too frequently and which does not have any associated positive or negative gain with it. Future studies will have to address how associative and nonassociative plasticity mechanisms interact to prevent repeated but reinforced stimuli to be less represented in a mixture.

Our work, as well as other studies of plasticity in early sensory processing (Faber *et al.*, 1999; Daly & Smith, 2000; Sandoz *et al.*, 2003; Yu *et al.*, 2004; Sachse *et al.*, 2007; Das *et al.*, 2011), raises two important questions that now need to be addressed. First, what modulatory pathway, if any, is involved in modulation of synapses to accomplish the nonassociative plasticity we have described? The computational model that we used did not implement a modulatory pathway. However, there are several possibilities for modulatory circuits. The biogenic amines octopamine and dopamine have been implicated in associative conditioning of appetitive (sucrose) and aversive (electroshock) stimuli in the honey bee and fruit fly brains (Hammer, 1997; Farooqui *et al.*, 2003; Schwaerzel *et al.*, 2003; Vergoz *et al.*, 2007). It may therefore be that these or other biogenic amines are involved in nonassociative conditioning. Furthermore, NMDA receptors have been identified in the honey bee brain (Zannat *et al.*, 2006) and have been shown to be involved in plasticity that underlies odor-specific habituation in the *Drosophila* AL (Das *et al.*, 2011). Nitric oxide is also present in insect ALs and may be involved in synaptic plasticity (Muller & Hildebrandt, 2002).

The second important question regards how other areas of the brain interact with or even help drive plasticity in the AL. We have shown that the representation of the exposed odor does not change as a result of odor exposure, yet our earlier behavioral studies have shown that the behavior toward the exposed odor changes (Chandra *et al.*, 2010). Therefore, plasticity in the AL alone cannot completely account for latent inhibition. For this reason we propose that the AL only provides an initial filtering, or preprocessing, of the signal that in some as-yet unspecified way helps downstream processing. But this raises the question of the relationship between plasticity in the AL and plasticity in other areas of the brain, and whether what we have measured even originates in the AL. Several lines of argument support the conclusion that the plasticity we have identified could reside in the AL itself. Studies in the fruit fly (Sachse *et al.*, 2007; Das *et al.*, 2011) have shown that some components of the plasticity reside at LN-to-PN synapses in the AL. Furthermore, activation of different signaling pathways in the AL is crucial for different forms of olfactory memory (Grünbaum & Müller, 1998; Müller, 2000; Müller & Hildebrandt, 2002; Ashraf *et al.*, 2006; Thum *et al.*, 2007), and structural plasticity in the AL as a consequence of olfactory experience has been shown in Winnington *et al.*, 1996; Sigg *et al.*, 1997; Devaud *et al.*, 2001; Sachse *et al.*, 2007; Hourcade *et al.*, 2009 and Das *et al.*, 2011. Finally, our model suggests that the kind of nonassociative learning that we are

studying here can be achieved by the sole participation of the intrinsic elements of the AL network (i.e. ORNs, LNs and PNs) combined with Hebbian plasticity.

However, we cannot rule out that the changes underlying plasticity in the AL could be influenced by feedback from other brain areas. Feedback neurons from the mushroom bodies to the ALs have been reported in the fruit fly (Hu *et al.*, 2010) and honey bee (Rybäk & Menzel, 1993 Kirschner *et al.*, 2006). Any feedback from the mushroom bodies to the AL that would account for the plasticity we have identified would need to be selective to provide modulation of odor-specific PNs. The current anatomical description of the feedback pathway in the honey bee involves a single, or at most a few, neurons that make broad connections across glomeruli in the AL. Therefore, any modulation would seem to be broad-based and lack the needed specificity to account for our data. Nevertheless, future studies should be focused on describing the specific origin and target of feedback neurons, and it will be important to establish whether the changes we observe in the AL are necessary and/or sufficient for producing the behavioral effect reported here. Indeed, changes in the visual context affect behavioral expression of latent inhibition (Chandra *et al.*, 2010). It would be interesting to establish whether alteration of the visual context changes expression of latent inhibition in the AL, which would most likely occur via feedback.

In summary, we now know that there are subtle changes in the AL activity due to unsupervised learning that filters the most common information. Combining modeling with empirical work has benefitted our study by providing specific explanations for why the changes occur, from both a mechanistic and a theoretical basis. It has provided us with several new testable hypotheses for future work. The answer to these questions will no doubt require further combined empirical and computation modeling studies.

## Acknowledgements

Thanks to Mathias Ditzen for providing analytical software. This research was funded by the NIH NCRR grant RR014166 to B.H.S., NIDCD grant DC007997 to B.H.S. and NIDCD grant DC011422 (to R.H., B.H.S. and M. Bazhenov) and also by grant BMBF 01GQ0771 from the German Research Ministry to C.G.G. None of the authors have a conflict of interest for this work.

## Abbreviations

AL, antennal lobe; EAG, electroantennogram; LN, local neuron; ORN, olfactory receptor neuron; PC, principal component; PCA, principal component analysis; PN, projection neuron.

## References

- Abel, R., Rybak, J. & Menzel, R. (2001) Structure and response patterns of olfactory interneurons in the honeybee, *Apis mellifera*. *J. Comp. Neurol.*, **437**, 363–383.
- Ashraf, S.I., McLoon, A.L., Scarsic, S.M. & Kunes, S. (2006) Synaptic protein synthesis associated with memory is regulated by the RISC pathway in Drosophila. *Cell*, **124**, 191–205.
- Bazhenov, M., Stopfer, M., Rabinovich, M., Abarbanel, H.D., Sejnowski, T.J. & Laurent, G. (2001) Model of cellular and network mechanisms for odor-evoked temporal patterning in the locust antennal lobe. *Neuron*, **30**, 569–581.
- Bitterman, M.E., Menzel, R., Fietz, A. & Schafer, S. (1983) Classical conditioning of proboscis extension in honeybees (*Apis mellifera*). *J. Comp. Psychol.*, **97**, 107–119.
- Chandra, S.B., Wright, G.A. & Smith, B.H. (2010) Latent inhibition in the honey bee, *Apis mellifera*: is it a unitary phenomenon? *Anim. Cogn.*, **13**, 805–815.
- Cleland, T.A., Morse, A., Yue, E.L. & Linster, C. (2002) Behavioral models of odor similarity. *Behav. Neurosci.*, **116**, 222–231.
- Daly, K.C. & Smith, B.H. (2000) Associative olfactory learning in the moth *Manduca sexta*. *J. Exp. Biol.*, **203**, 2025–2038.
- Daly, K., Christensen, T.A., Lei, H., Smith, B.H. & Hildebrand, J.G. (2004) Learning modulates the ensemble representations for odors in primary olfactory networks. *Proc. Natl. Acad. Sci. USA*, **101**, 10476–10481.
- Das, S., Sadanandappa, M.K., Dervan, A., Larkin, A., Lee, J.A., Sudhakaran, I.P., Priya, R., Heidari, R., Holohan, E.E., Pimentel, A., Gandhi, A., Ito, K., Sanyal, S., Wang, J.W., Rodrigues, V. & Ramaswami, M. (2011) Plasticity of local GABAergic interneurons drives olfactory habituation. *Proc. Natl. Acad. Sci. USA*, **108**, 646–654.
- Deisig, N., Giurfa, M., Lachnit, H. & Sandoz, J.C. (2006) Neural representation of olfactory mixtures in the honeybee antennal lobe. *Eur. J. Neurosci.*, **24**, 1161–1174.
- Deisig, N., Giurfa, M. & Sandoz, J.C. (2010) Antennal lobe processing increases separability of odor mixture representations in the honeybee. *J. Neurophysiol.*, **103**, 2185–2194.
- Denker, M., Finke, R., Schaupp, F., Grun, S. & Menzel, R. (2010) Neural correlates of odor learning in the honeybee antennal lobe. *Eur. J. Neurosci.*, **31**, 119–133.
- Destexhe, A., Mainen, Z.F. & Sejnowski, T.J. (1994) Synthesis of models for excitable membranes, synaptic transmission and neuromodulation using a common kinetic formalism. *J. Comput. Neurosci.*, **1**, 195–230.
- Devaud, J.M., Acebes, A. & Ferrús, A. (2001) Odor exposure causes central adaptation and morphological changes in selected olfactory glomeruli in Drosophila. *J. Neurosci.*, **21**, 6274–6282.
- Distler, P.G., Gruber, C. & Boeckh, J. (1998) Synaptic connections between GABA-immunoreactive neurons and uniglomerular projection neurons within the antennal lobe of the cockroach, *Periplaneta americana*. *Synapse*, **29**, 1–13.
- Faber, T., Joerges, J. & Menzel, R. (1999) Associative learning modifies neural representations of odors in the insect brain. *Nat. Neurosci.*, **2**, 74–78.
- Farooqui, T., Robinson, K., Vaessin, H. & Smith, B.H. (2003) Modulation of early olfactory processing by an octopaminergic reinforcement pathway in the honeybee. *J. Neurosci.*, **23**, 5370–5380.
- Fdez Galán, R., Sachse, S., Galizia, C.G. & Herz, A.V. (2004) Odor-driven attractor dynamics in the antennal lobe allow for simple and rapid olfactory pattern classification. *Neural Comput.*, **16**, 999–1012.
- Fernandez, P.C., Locatelli, F.F., Person-Rennell, N., Deleo, G. & Smith, B.H. (2009) Associative conditioning tunes transient dynamics of early olfactory processing. *J. Neurosci.*, **29**, 10191–10202.
- Flanagan, D. & Mercer, A.R. (1989) An atlas and 3-D reconstruction of the antennal lobes in the worker honey bee, *Apis mellifera* (Hymenoptera, Apidae). *Int. J. Insect Morphol. Embryol.*, **18**, 145–159.
- Galan, R.F., Weidert, M., Menzel, R., Herz, A.V. & Galizia, C.G. (2006) Sensory memory for odors is encoded in spontaneous correlated activity between olfactory glomeruli. *Neural Comput.*, **18**, 10–25.
- Galizia, C.G. & Vetter, R. (2004) Optical methods for analyzing odor-evoked activity in the insect brain. In Christensen, T.A. (Ed.), *Advances in Insect Sensory Neuroscience*. CRC Press, Boca Raton, FL, pp. 349–392.
- Galizia, C.G., McIlwrath, S.L. & Menzel, R. (1999) A digital three-dimensional atlas of the honeybee antennal lobe based on optical sections acquired by confocal microscopy. *Cell Tissue Res.*, **295**, 383–394.
- Grünbaum, L. & Müller, U. (1998) Induction of a specific olfactory memory leads to a long-lasting activation of protein kinase C in the antennal lobe of the honeybee. *J. Neurosci.*, **18**, 4384–4392.
- Guerrieri, F., Schubert, M., Sandoz, J.C. & Giurfa, M. (2005) Perceptual and neural olfactory similarity in honeybees. *PLoS Biol.*, **3**, e60.
- Hammer, M. (1997) The neural basis of associative reward learning in honeybees. *Trends Neurosci.*, **20**, 245–252.
- Hildebrand, J.G. & Shepherd, G.M. (1997) Mechanisms of olfactory discrimination: converging evidence for common principles across phyla. *Annu. Rev. Neurosci.*, **20**, 595–631.
- Hourcade, B., Perisse, E., Devaud, J.M. & Sandoz, J.C. (2009) Long-term memory shapes the primary olfactory center of an insect brain. *Learn. Mem.*, **16**, 607–615.
- Hu, A., Zhang, W. & Wang, Z. (2010) Functional feedback from mushroom bodies to antennal lobes in the Drosophila olfactory pathway. *Proc. Natl. Acad. Sci. USA*, **107**, 10262–10267.
- Huerta, R. & Rabinovich, M. (2004) Reproducible sequence generation in random neural ensembles. *Phys. Rev. Lett.*, **93**, 238104.
- Huerta, R., Sánchez-Montaños, M.A., Corbacho, F. & Sigüenza, J.A. (2000) A central pattern generator to control a pyloric-based system. *Biol. Cybern.*, **82**, 85–94.
- Hunter, A.J. & Murray, T.K. (1989) Cholinergic mechanisms in a simple test of olfactory learning in the rat. *Psychopharmacology*, **99**, 270–275.

- Joerges, J., Küttner, A., Galizia, C.G. & Menzel, R. (1997) Representation of odours and odour mixtures visualized in the honeybee brain. *Nature*, **387**, 285–288.
- Kirschner, S., Kleineidam, C.J., Zube, C., Rybak, J., Grünwald, B. & Rössler, W. (2006) Dual olfactory pathway in the honeybee, *Apis mellifera*. *J. Comp. Neurosci.*, **499**, 933–952.
- Linster, C., Menon, A.V., Singh, C.Y. & Wilson, D.A. (2009) Odor-specific habituation arises from interaction of afferent synaptic adaptation and intrinsic synaptic potentiation in olfactory cortex. *Learn. Mem.*, **16**, 452–459.
- Lubow, R.E. (1973) Latent inhibition. *Psychol. Bull.*, **79**, 398–407.
- Mauelshagen, J. (1993) Neural correlates of olfactory learning paradigms in an identified neuron in the honeybee brain. *J. Neurophysiol.*, **69**, 609–625.
- Mazor, O. & Laurent, G. (2005) Transient dynamics versus fixed points in odor representations by locust antennal lobe projection neurons. *Neuron*, **48**, 661–673.
- Müller, U. (2000) Prolonged activation of cAMP-dependent protein kinase during conditioning induces long-term memory in honeybees. *Neuron*, **27**, 159–168.
- Müller, U. & Hildebrandt, H. (2002) Nitric oxide/cGMP-mediated protein kinase A activation in the antennal lobes plays an important role in appetitive reflex habituation in the honeybee. *J. Neurosci.*, **22**, 8739–8747.
- Peele, P., Ditzén, M., Menzel, R. & Galizia, C.G. (2006) Appetitive odor learning does not change olfactory coding in a subpopulation of honeybee antennal lobe neurons. *J. Comp. Physiol. A Neuroethol. Sens. Neural. Behav. Physiol.*, **192**, 1083–1103.
- Rath, L., Galizia, C.G. & Szyszka, P. (2011) Multiple memory traces after associative learning in the honey bee antennal lobe. *Eur. J. Neurosci.*, **34**, 352–360.
- Rybak, J. & Menzel, R. (1993) Anatomy of the mushroom bodies in the honey bee brain: the neuronal connections of the alpha-lobe. *J. Comp. Neurol.*, **334**, 444–465.
- Sachse, S. & Galizia, C.G. (2002) Role of inhibition for temporal and spatial odor representation in olfactory output neurons: a calcium imaging study. *J. Neurophysiol.*, **87**, 1106–1117.
- Sachse, S. & Galizia, C.G. (2003) The coding of odour-intensity in the honeybee antennal lobe: local computation optimizes odour representation. *Eur. J. Neurosci.*, **18**, 2119–2132.
- Sachse, S., Rappert, A. & Galizia, C.G. (1999) The spatial representation of chemical structures in the antennal lobe of honeybees: steps towards the olfactory code. *Eur. J. Neurosci.*, **11**, 3970–3982.
- Sachse, S., Rueckert, E., Keller, A., Okada, R., Tanaka, N.K., Ito, K. & Vosshall, L.B. (2007) Activity-dependent plasticity in an olfactory circuit. *Neuron*, **56**, 838–850.
- Sandoz, J.C., Galizia, C.G. & Menzel, R. (2003) Side-specific olfactory conditioning leads to more specific odor representation between sides but not within sides in the honeybee antennal lobes. *Neuroscience*, **120**, 1137–1148.
- Schwaerzel, M., Monastirioti, M., Scholz, H., Friggi-Grelin, F., Birman, S. & Heisenberg, M. (2003) Dopamine and octopamine differentiate between aversive and appetitive olfactory memories in Drosophila. *J. Neurosci.*, **23**, 10495–10502.
- Shannon, C.F. (1948) A mathematical theory of communication. *Bell Syst. Tech. J.*, **27**, 379–423.
- Sigg, D., Thompson, C.M. & Mercer, A.R. (1997) Activity-dependent changes to the brain and behavior of the honey bee, *Apis mellifera* (L.). *J. Neurosci.*, **17**, 7148–7156.
- Smith, B.H. (1996) The role of attention in learning about odorants. *Biol. Bull.*, **191**, 76–83.
- Smith, B.H. (1998) Analysis of interaction in binary odorant mixtures. *Physiol. Behav.*, **65**, 397–407.
- Smith, B.H., Wright, G.A. & Daly, K.S. (2006) Learning-based recognition and discrimination of floral odors. In Dudareva, N. & Pichersky, E. (Eds), *The Biology of Floral Scents*. CRC Press, Boca Raton, FL, pp. 263–295.
- Stopfer, M. & Laurent, G. (1999) Short-term memory in olfactory network dynamics. *Nature*, **402**, 664–668.
- Strausfeld, N.J. & Hildebrand, J.G. (1999) Olfactory systems: common design, uncommon origins? *Curr. Opin. Neurobiol.*, **9**, 634–639.
- Szücs, A., Huerta, R., Rabinovich, M.I. & Selverston, A.I. (2009) Robust microcircuit synchronization by inhibitory connections. *Neuron*, **61**, 439–453.
- Thum, A.S., Jenett, A., Ito, K., Heisenberg, M. & Tanimoto, H. (2007) Multiple memory traces for olfactory reward learning in Drosophila. *J. Neurosci.*, **27**, 11132–11138.
- Vergoz, V., Roussel, E., Sandoz, J.C. & Giurfa, M. (2007) Aversive learning in honeybees revealed by the olfactory conditioning of the sting extension reflex. *PLoS ONE*, **2**, e288.
- Wilson, D.A. & Linster, C. (2008) Neurobiology of a simple memory. *J. Neurophysiol.*, **100**, 2–7.
- Wilson, H.R. & Cowan, R.D. (1972) Excitatory and Inhibitory interactions in localized populations of model neurons. *J. Biophys.*, **12**, 1–24.
- Wilson, R.I., Turner, G.C. & Laurent, G. (2004) Transformation of olfactory representations in the Drosophila antennal lobe. *Science*, **303**, 366–370.
- Winnington, A.P., Napper, R.M. & Mercer, A.R. (1996) Structural plasticity of identified glomeruli in the antennal lobes of the adult worker honey bee. *J. Comp. Neurol.*, **365**, 479–490.
- Yu, D., Ponomarev, A. & Davis, R.L. (2004) Altered representation of the spatial code for odors after olfactory classical conditioning; memory trace formation by synaptic recruitment. *Neuron*, **42**, 437–449.
- Zannat, M.T., Locatelli, F., Rybak, J., Menzel, R. & Leboulle, G. (2006) Identification and localisation of the NR1 sub-unit homologue of the NMDA glutamate receptor in the honeybee brain. *Neurosci. Lett.*, **398**, 274–279.